Biogeochemical model of CO_2 and CH_4 production in anoxic Arctic soil microcosms

Guoping Tang[1], Jianqiu Zheng[2], Xiaofeng Xu[3], Ziming Yang[1], David E. Graham[2,4], Baohua Gu[1], Scott Painter[1,4], and Peter E. Thornton[1,4]

[1]Environmental Sciences Division, Oak Ridge National Laboratory, Oak Ridge TN, 37831 USA
[2]Biosciences Sciences Division, Oak Ridge National Laboratory, Oak Ridge TN, 37831 USA
[3]Biology Department, San Diego State University, San Diego, CA, 92182 USA
[4]Climate Change Science Institute, Oak Ridge National Laboratory, Oak Ridge TN, 37831 USA

Correspondence to: Guoping Tang (guopingtangva@gmail.com)

Abstract. Soil organic carbon turnover to CO_2 and CH_4 is sensitive to soil redox potential and pH conditions. However, land surface models do not consider redox and pH in the aqueous phase explicitly, thereby limiting their use for making predictions in anoxic environments. Using recent data from incubations of Arctic soils, we extend the Community Land Model Carbon Nitrogen (CLM-CN) decomposition cascade to include simple organic substrate turnover, fermentation, Fe(III) reduction, and methanogenesis reactions, and assess the efficacy of various temperature and pH response functions. Incorporating the Windermere Humic Aqueous Model (WHAM) enables us to approximately describe the observed pH evolution without additional parameterization. Although Fe(III) reduction is normally assumed to compete with methanogenesis, the model predicts that Fe(III) reduction raises the pH from acidic to neutral, thereby reducing environmental stress to methanogens and accelerating methane production when substrates are not limiting. The equilibrium speciation predicts a substantial increase in CO_2 solubility as pH increases, and taking into account CO_2 adsorption to surface sites of metal oxides further decreases the predicted headspace gas-phase fraction at low pH. Without adequate representation of these speciation reactions, and the impact of pH, temperature, and pressure, CO_2 production from closed microcosms can be substantially underestimated based on headspace CO_2 measurements only. Our results demonstrate the efficacy of geochemical models for simulating soil biogeochemistry and provide predictive understanding and mechanistic representations that can be tested in land surface models to improve climate model predictions.

Key words. anaerobic incubation, Fe(III) reduction, methanogenesis, pH, temperature response

1 Introduction

Projected increases in temperature and soil saturation and vegetation shift are widely expected to accelerate the release of the large amount of soil organic matter (SOM) stored in the Arctic as CO_2 and CH_4 into the atmosphere, which may form a positive feedback to climate change (Treat et al., 2015;Knoblauch et al., 2013;Elberling et al., 2013). SOM decomposition models are developed mostly for aerobic conditions (Manzoni and Porporato, 2009) and are modified for use under anaerobic conditions. For example, the Community Land Model Carbon Nitrogen (CLM-CN) decomposition cascade is used to implicitly represent anaerobic decomposition with a moisture response function that approaches unity at saturation and an oxygen scalar that has a large unresolved uncertainty (Oleson et al., 2013). In a recent permafrost carbon climate feedback modeling study, the carbon release rate from permafrost soils after thawing under aerobic conditions was assumed to be 3.4 times higher than the release rate under anaerobic conditions (Koven et al., 2015;Schädel et al., 2016). However, in incubations with soils from Alaska and Siberia, carbon release under aerobic conditions was 3.9–10 times greater than release under anaerobic conditions (Lee et al., 2012), indicating that these existing models do not adequately represent the anaerobic processes for accurate prediction of SOM turnover and heterotrophic respiration.

Because CH_4 has a 100-year global warming potential that is about 26 times greater than CO_2 (Forster et al., 2007;IPCC, 2013), it is important to accurately represent methanogenesis in the context of competing anaerobic processes. Methanogenesis is carried out by a group of strictly anaerobic Archaea. The free energy of methanogenesis reactions is less favorable than the reduction of O_2, NO_3^-, Mn (IV), Fe(III), and SO_4^{2-} along the redox ladder (Conrad, 1996;Bethke et al., 2011). The accumulation of CH_4 has been widely observed to lag behind CO_2 for periods ranging from days to years in incubations (Knoblauch et al., 2013;Roy Chowdhury et al., 2015;Cui et al., 2015;Hoj et al., 2007;Fey et al., 2004;Jerman et al., 2009;Tang et al., 2013c). Besides temperature (Fey and Conrad, 2003;Hoj et al., 2007;Jerman et al., 2009;Cui et al., 2015) and initial methanogen abundance (Conrad, 1996;Knoblauch et al., 2013), the wide range of redox buffers provided by the alternative electron acceptors is likely a cause of the wide range of lag times that has been observed (Estop-Aragonés and Blodau, 2012;Fey et al., 2004;Jerman et al., 2009;Yao et al., 1999;Conrad, 1996;Knorr and Blodau, 2009). As a result, the ratio of CH_4 to CO_2 ranges from 0.00001 to 0.5 (Wania et al., 2010;Drake et al., 2009;Bridgham et al., 2013). Nevertheless, some land surface models (LSM) parameterize methanogenesis as a fraction of carbon mineralization (Wania et al., 2013;Oleson et al., 2013;Koven et al., 2015;Tian et al., 2015;Cheng et al., 2013). While methanogenesis is explicitly represented in some models (Xu et al., 2015;Grant, 1998) and the reduction of alternative electron acceptors is explicitly represented in others (Fumoto et al., 2008;Segers and Kengen, 1998;Van Bodegom et al., 2001;van Bodegom et al., 2000), these models do not have an aqueous phase that is essential for explicit biogeochemical calculations. Because methanogenesis is sensitive to redox conditions, the lack of explicit biogeochemical representation of the redox processes contributes to the prediction uncertainty of CH_4 emission.

Anaerobic bacteria and Archaea usually depend on simple substrates such as sugars, alcohols, organic acids, and H_2 as carbon and energy sources, sources that are rarely simulated in ecosystem models. The abundance and importance of dissolved organic matter (DOM) and low-molecular-weight organic carbon (LMWOC) in SOM turnover in the Arctic soils are becoming increasingly recognized (Hodgkins et al., 2014). The DOM concentration in water flowing from collapsing

5 permafrost (thermokarsts) on the North Slope of Alaska ranges from 0.2−8 mM, with biodegradable (degrade in 40 d) DOM accounting for 10-60 % (Abbott et al., 2014;Arnosti, 1998, 2000;Arnosti et al., 1998). Ancient LMWOC was found to fuel rapid CO_2 production upon thawing (Drake et al., 2015). On the other hand, new SOM consists of mostly macromolecules of plant and microbial residues such as carbohydrates (polysaccharides, including cellulose, hemicellulose, lignin, etc.), lipids, nucleic acids, and proteins (Kögel-Knabner, 2002). While conceptual models and measurements connecting SOM with

10 LMWOC have long existed (Drake et al., 2009;Tveit et al., 2013;Tveit et al., 2015;Bridgham et al., 2013), the hydrolysis and fermentation reactions have been poorly quantified. Among the over 250 SOM decomposition models that have been developed in the past 80 years (Manzoni and Porporato, 2009), only a few models explicitly simulate simple substrates (Xu et al., 2016b). Either a simple carbon pool (Cao et al., 1995;Cao et al., 1998;Kettunen, 2003) or a DOM pool (Tian et al., 2010;Xu and Tian, 2012) has been assumed for methanogenesis. Acetate and H_2 have been added with their production

15 parameterized as a function of carbon mineralization (Van Bodegom et al., 2001;van Bodegom et al., 2000;Grant, 1998;Xu et al., 2015). It is not surprising that CH_4 production prediction is sensitive to simple substrate production (Kettunen, 2003;Weedon et al., 2013). While detailed SOM decomposition models include depolymerization to produce monomers under aerobic conditions (Riley et al., 2014), production and consumption of simple measurable substrates, such as acetate, H_2, formate, etc., are not represented under anaerobic conditions.

In addition to electron acceptors and substrates, SOM turnover is also sensitive to soil pH. Most methanogens grow over a relatively narrow pH range (6-8), while some adapt to acidic or basic environments (Garcia et al., 2000;Van Kessel and Russell, 1996;Wang et al., 1993;Sowers et al., 1984;Rivkina et al., 2007;Hao et al., 2012;Kotsyurbenko et al., 2004;Kotsyurbenko et al., 2007). The pH response functions in LSMs are empirical and vary substantially (Xu et al., 2016b).

25 Because of the large buffer capacity, soil pH is often fixed in LSMs (Oleson et al., 2013;Tian et al., 2010). But in reality, pH does change 1-2 logarithm units in laboratory incubations (Xu et al., 2015;Roy Chowdhury et al., 2015;Peters and Conrad, 1996;Drake et al., 2015) and in the field, where it can vary significantly through the soil profile and along topographic and vegetation gradients (Cao et al., 1995;Van Bodegom et al., 2001;Lipson et al., 2013b). pH is calculated using soil acidity and soil buffer capacity (Van Bodegom et al., 2001) or as a function of acetate concentration (Xu et al., 2015). It is desirable to

30 use a geochemical model to describe pH evolution mechanistically.

SOM turnover is also sensitive to temperature. The reported Q_{10} values for methanogen temperature response vary from 1.5 to 4 (Xu et al., 2016b). Methanogenesis has been widely observed to diminish when the temperature decreases toward 0 °C (Dunfield et al., 1993;Fey et al., 2004;Hoj et al., 2007;Sowers et al., 1984), predicting little CH_4 production from the surface

layers of frozen Arctic soils. However, recent observations suggest that CH_4 emissions during the winter season account for $\geq 50\%$ of the annual emission in the Arctic (Zona et al., 2016). The cold season CH_4 production is among the most uncertain processes for predicting seasonal CH_4 cycle in northern wetlands (Xu et al., 2016a). The temperature response functions need to be assessed as well.

Overall, anaerobic SOM turnover is controlled by the hydrolysis of the macromolecules to produce simple substrates and the sequential microbial reduction of electron acceptors along the redox ladder. Because SOM turnover and CO_2 and CH_4 production are sensitive to redox potential, pH, and temperature, it is desirable to simulate the redox and pH explicitly with geochemical models. With the accumulation of new data on metabolic intermediates, electron acceptors, greenhouse gases, and pH from incubations with Arctic soils at various temperatures (Drake et al., 2015;Herndon et al., 2015a;Herndon et al., 2015b;Yang et al., 2016;Mann et al., 2015), our objectives are to integrate these new data into geochemical models to (1) extend the CLM-CN decomposition cascade to include simple substrates such as sugars and organic acids and add Fe(III) reduction and methanogenesis processes, (2) account for gas, aqueous, and adsorbed phase speciation, (3) describe pH mechanistically, and (4) assess the existing temperature and pH response functions. Unlike previous LSMs, we simulate speciation of CO_2 and CH_4 in the gas, aqueous, and solid phases, and represent sugars, organic acids, Fe(II), Fe(III), Fe reducers, and methanogens, and account for both thermodynamic and kinetic control. Our results provide predictive understanding and mechanistic representations that can be tested in other LSMs, e.g., CLM-PFLOTRAN (Tang et al., 2016), to improve climate model predictions.

2 Materials and methods

We extend the CLM-CN decomposition cascade (Thornton and Rosenbloom, 2005) by adding reactions for hydrolysis to produce sugars, fermentation to produce organic acids and H_2 (Grant, 1998;Xu et al., 2015), Fe(III) reduction, and methanogenesis reactions (Tang et al., 2013c). We add the Windermere Humic Aqueous Model (WHAM) (Tipping, 1994) to simulate the pH buffer by SOM. Recent microcosm data (Herndon et al., 2015a;Roy Chowdhury et al., 2015) are used to assess these representations. While nitrogen (ammonium and nitrate) concentrations can affect carbon mineralization (Lavoie et al., 2011), we do not account for this effect because of a lack of nitrogen measurements from these experiments.

2.1 Soil incubation experiment data

The materials, experimental procedures and results for the microcosm tests were reported previously (Herndon et al., 2015a;Roy Chowdhury et al., 2015). Briefly, three soil cores were taken from center, ridge, and trough locations in a low-center polygon in the wet tundra of the Barrow Environmental Observatory in Alaska. Soil samples from the organic and mineral horizons of the three cores were analyzed for gravimetric water content, pH, Fe(II), water-extractable organic carbon (WEOC), organic acids, and total carbon content (TOTC). For each horizon and location, about 15 g of homogenized wet

soil was placed into a 60 ml sterile serum bottle, which was sealed and flushed with pure N_2 gas. The microcosms were incubated at -2, 4, and 8 °C for about 2 months to mimic thawing during the summer season at the site. The headspace CO_2 and CH_4 were sampled and analyzed by gas chromatography. Separate microcosms with 20 g of the homogenized soils were incubated to analyze for pH, Fe(II), WEOC, and organic acids. Additional soil characterization is available elsewhere

5   (Bockheim et al., 2001;Lipson et al., 2010;Lipson et al., 2013b).

2.2 Model developments

2.2.1 SOM decomposition

The SOM in the Arctic soils was characterized using high-resolution mass spectroscopy (Herndon et al., 2015a;Mann et al.,

10   2015;Hodgkins et al., 2014). However, these characterizations were insufficient to partition SOM into many chemically distinct organic pools (Riley et al., 2014;Kögel-Knabner, 2002). Therefore, we extend the CLM-CN decomposition cascade to produce intermediate metabolites (Fig. 1). To limit the number of new pools, we lump reducing sugars, alcohols, etc. (Yang et al., 2016;Kotsyurbenko et al., 1993;Glissmann and Conrad, 2002;Tveit et al., 2015) into a LabileDOC pool, and the organic acids, such as formate, acetate, propionate, and butyrate, etc. (Herndon et al., 2015a;Kotsyurbenko et al., 1993;Peters

15   and Conrad, 1996;Tveit et al., 2015) into an organic acid pool (Ac) (Xu et al., 2015;Grant, 1998). Assuming that the LabileDOC turns over in 20 h as the Lit1 pool in CLM-CN (Thornton and Rosenbloom, 2005) or glucose fermentation (Rittmann and McCarty, 2001), we split the original respiration factor into a direct and an indirect fraction, with the indirect fraction s_{labile} to produce LabileDOC, which respires through the anaerobic pathway (Fig. 1) to CO_2 or CH_4, and the direct respiration fraction (1- s_{labile}) respires directly to CO_2. We estimate s_{labile} by comparing the predictions with the observations

20   in this work. The fermentation reaction is (Xu et al., 2015;Grant, 1998;van Bodegom and Scholten, 2001;Madigan, 2012)

$$C_6H_{12}O_6 + 4 H_2O => 2 CH_3COO^- + 2 HCO_3^- + 4 H^+ + 4 H_2, \tag{R1}$$

which lowers the pH and further respires $s_{labile}/3$ of SOM into CO_2.

2.2.2 Fe(III) reduction, methanogenesis, and biomass decay

Because Fe(III) reduction contributes 40-45 % of the ecosystem respiration in some Arctic sites (Lipson et al., 2013b) and

25   NO_3^- and SO_4^{2-} concentrations are typically low in the experiments, we add Fe(III) reduction reactions to represent the reduction of alternative electron acceptors to O_2. We use the microbial reactions formed by combining electron donor (oxidation) half reactions, electron acceptor (reduction) half reactions, and cell synthesis reactions following bioenergetics (Rittmann and McCarty, 2001). Specifically, the Fe(III) reduction reactions are (Istok et al., 2010)

$$2.1 H_2O + NH_4^+ + 150.2 Fe^{3+} + 21.3 CH_3COO^- => C_5H_7O_2N + 150.2 Fe^{2+} + 167.4 H^+ + 37.5 HCO_3^-, \tag{R2}$$

30   $$5 HCO_3^- + NH_4^+ + 114.8 Fe^{3+} + 57.4 H_2 => C_5H_7O_2N + 114.8 Fe^{2+} + 110.8 H^+ + 13 H_2O, \tag{R3}$$
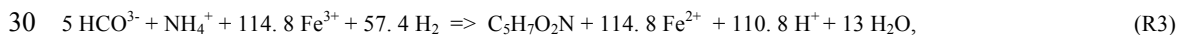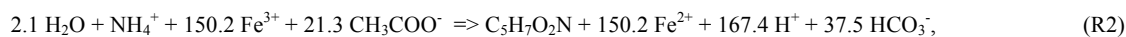
where, $C_5H_7O_2N$ represents microbial (iron reducer) mass, and NH_4^+ is assumed not to be limiting (at 1 μM). These two

reactions result in dissolution of ferric oxides, for example, $Fe(OH)_{3a}$, to release OH^- to increase pH. The rate is

$$\frac{dx}{dt} = k_{\max}x \frac{k_{surf}}{k_{surf}+x/m_{surf,avail}} \frac{m_D}{k_D+m_D} f(G), \tag{1}$$

where $k_{\max}$ is the kinetic rate constant; x is concentration of biomass; $m_{surf,avail}$ is the microbially-available surface sites

5   taken as the $Fe(OH)_{3a}$ surface sites Hfo associated with H^+, i.e., $m_{surf,avail} = m_{Hfo\_wOH} + m_{Hfo\_sOH}$ in moles per liter pore

fluid; k_{surf} accounts for the impact of $x/m_{surf,avail}$, which represents the interaction of biomass with available Fe(III) sites

on the surface; m_D and k_D are the concentration and half saturation of the electron donors (acetate or H_2); and $f(G)$ is a

thermodynamic factor that goes to zero when the reaction is thermodynamically unfavourable (Jin and Roden, 2011).

The methanogenesis reactions are (Istok et al., 2010)

10    $1.5 H^+ + 98.2 H_2O + NH_4^+ + 103.7 CH_3COO^- => C_5H_7O_2N + 101.2 HCO_3^- + 101.2 CH_4$, (R4)

$84.9 H^+ + NH_4^+ + 85.9 HCO_3^- + 333.5 H_2 => C_5H_7O_2N + 255.6 H_2O + 80.9 CH_4$. (R5)
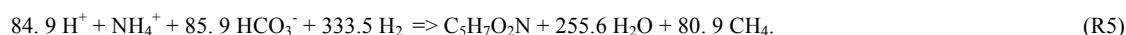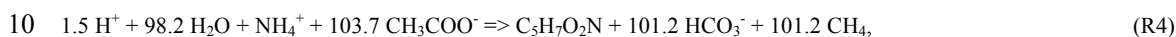
These two reactions consume protons to increase pH. The rate is

$$\frac{dx}{dt} = k_{max}x \frac{m_D}{k_D+m_D} f(G). \tag{2}$$

We use one pool FeRB for the iron reducers and separate the methanogens into MeGA and MeGH pools for acetoclastic and

15   hydrogenotrophic methanogens (Fig. 1). The biomass decay reaction for FeRB, MeGA, and MeGH is

$0.2 C_5H_7O_2N => 0.1 SOM1 + 0.2 SOM2 + 0.25 SOM3 + 0.45 SOM4 + 0.1185 NH_4^+ + …$. (R6)
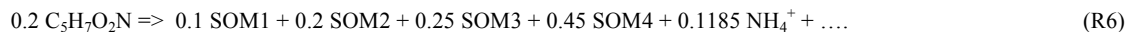
Like the SOM pools, the rate is first order.

2.2.3 pH

The soil pH is typically buffered by carbonates, clay minerals, metal oxides, and organic matter (Tipping, 1994;Tang et al.,

20   2013a). The Windermere Humic Aqueous Model (WHAM) is used to approximate SOM as humic acid and fulvic acid, with

a number of monodentate and bidentate binding sites for protons, to describe the pH buffering due to SOM (Tipping, 1994).

The surface complexation model for ferrihydrate is used to describe the sorption of carbonate and proton to metal oxides

(Dzombak and Morel, 1990). Additional aqueous speciation reactions are also included in the reaction database available as

supplemental information (also publicly available at https://github.com/t6g/bgcs).

25 2.2.4 pH and temperature response functions

We use the CLM4Me pH response function (Riley et al., 2011)

$$log_{10}f(pH) = -0.2235pH^2 + 2.7727pH - 8.6 \tag{3}$$

and the CLM-CN temperature response function (Thornton and Rosenbloom, 2005;Lloyd and Taylor, 1994)

$$\ln f(T) = 308.56 \left(\frac{1}{71.02} - \frac{1}{T - 227.13} \right). \tag{4}$$

The pH response functions used in DLEM (Tian et al., 2010) and TEM (Raich et al., 1991) and a few other models (Cao et al., 1995;Xu et al., 2015), as described in Appendix 1, and the CENTURY temperature response function, the Q_{10} equation, Arrhenius equation, and Ratkowsky equation, which are described in Appendix 2, are used for comparison.

5 **2.3 Implementation, parameterization, and initialization**

2.3.1 Implementation

To calculate the speciation among gas, aqueous, and solid phases under various temperature, pH, and pressure conditions and explicitly describe pH and redox buffer, we employ the widely used extensively tested geochemical code PHREEQC (Parkhurst and Appelo, 2013) to synthesize the experimental data to develop and parameterize mechanistic representations.

10 The implementation of CLM-CN reactions in a geochemical code is detailed elsewhere (Tang et al., 2016). Guidelines for implementation of the microbial reactions, surface complexation, WHAM, etc., in PHREEQC are available in the user manual (Parkhurst and Appelo, 2013).

2.3.2 Parameterization

The stoichiometric and kinetic rate parameters for the CLM-CN reaction network are specified in Fig. 1. The indirect
15 respiration faction s_{labile} is highly uncertain. We start with $s_{labile} = 0.4$, and check the sensitivity with $s_{labile} = 0.2$ and 0.6. For the decay of biomass, and growth of methanogens, we use the general parameter values in the literature (Rittmann and McCarty, 2001). The half saturation k_D and k_{surf} values are taken from published literature (Jin and Roden, 2011). The parameter values and the references are listed in Table 1.

2.3.3 Initialization

20 The basic experimental parameters are summarized in Table 2 and Table S1. The amount of water, headspace volume, and temperature are set at the experimental parameter values. The initial pH, organic acids (combined formate, acetate, propionate, and butyrate from Table S1 to Table 2) and Fe(II) concentration are specified as measured.

The measured TOTC includes seven carbon pools in the CLM-CN decomposition cascade, as well as simple substrates (such
25 as sugars, alcohols, organic acids), and biomass for FeRB, MeGA, MeGH, and other microbes. Because of the lack of reliable methods in partitioning the measured TOTC into these pools, we combine the Lit1 pool with LabileDOC, Lit2 with SOM1, and Lit3 with SOM2 pools as they have identical turnover times (Fig. 1). That is, we will split the initial TOTC (minus simple substrates) into LabileDOC, SOM1, SOM2, SOM3, SOM4, FeRB, MeGA, and MeGH pools, with fraction $f_{labileDOC}, f_{som1}, f_{som2}, f_{som3}, f_{ferb}, f_{mega}$, and f_{megh}. Because the experiments lasted for only 2 months, and predictions are often not
30 very sensitive to the initial biomass (Tang et al., 2013b;Tang et al., 2013c;Xu et al., 2015;Jin and Roden, 2011), the

predictions are expected to be sensitive to $f_{labileDOC}$, f_{som1}, and f_{som2} under the experimental conditions. With a turnover (mean residence) time of 0.2-0.5, 6-9, and >125 years for the fast, slow, and passive pools, respectively, less than 5 % was estimated for the fast pool for 121 individual samples from 23 high-latitude ecosystems located across the northern circumpolar permafrost zone (Schädel et al., 2014). Based on incubation tests with Siberian soils for over 1200 d, the initial

5 labile carbon pools were estimated to comprise 2.22 ± 1.19 and 0.64 ± 0.28 % of the TOTC with turnover times of 0.26±1.56 and 0.21±1.58 y under aerobic and anaerobic conditions, respectively (Knoblauch et al., 2013). We set $f_{labileDOC} = 0.0005$, $f_{som1} = 0.01$, $f_{som2} = 0.02$, $f_{som3} = 0.1$, $f_{mega} = f_{megh} = 0.5f_{ferb} = 10^{-6}$ [approximating with *E. coli* with a wet weight 10^{-12} g, 70 % water, and 50 % dry weight carbon (Madigan, 2012), each microbial cell contains ~1.25×10^{-14} mole C, this means ~10^{8} cells in 1 mole TOTC, which roughly approximates the range of reported values (Roy Chowdhury et al., 2015)].

Bioavailable ferric oxides are assumed to be in the form of Fe(OH)$_{3a}$, with initial concentration as a fraction f_{fe3} of the dry soil mass. Depending on the season and the age of the drained thawed lake basins, HCl extractable Fe(III) is reported to range between 100 and 700 g Fe(III) m^{-3} in the Barrow soils in a 24 cm soil profile (Lipson et al., 2013a). Using a weighted average of bulk density of 0.26, this translates to 0.2 to 1 % g Fe(III)/g dry soil mass. We start with $f_{fe3} = 0.005$. Fe(III)

15 reduction dissolves Fe(OH)$_{3a}$ and releases adsorbed protons on the mineral surface, which is described by the surface complexation model (Dzombak and Morel, 1990). The organic content for WHAM is set at TOTC. The initial total inorganic carbon (TIC) in the solution is assumed to be in equilibrium with an atmosphere of CO$_2$ at 400 ppm and 1 atm. The headspace gas starts with N$_2$ at 1 atm. These parameters are summarized in Table S2. Additional specifics are available in the scripts to produce input files. The reaction database [extended from (Tang et al., 2013b;Tang et al., 2013c)], the python

20 scripts to create input files for various locations, temperatures, and other options (e.g., temperature and pH response functions) and scripts used to make the figures are provided as supplemental information.

3 Results and discussion

3.1 Experimental observations

The experimental results of anoxic soil incubation experiments were published elsewhere (Herndon et al., 2015a;Roy

25 Chowdhury et al., 2015), so we briefly describe the original observed headspace CO$_2$ and CH$_4$ concentration, soil Fe(II) and organic acids concentration, and pH (Fig. 2). The overall observations appear to separate between the soil horizons (organic vs. mineral soils) rather than among the microtopographic locations (center, ridge, and trough) of ice-wedge polygons. Up to 20 % CO$_2$ was observed in the headspace by the end of the 2-month incubations, with higher concentrations in the organic soils than in the mineral soils (Fig. 2a1-3 vs. 4-6). This can be attributed to the higher organic content of the organic soils

30 compared to that of the mineral soils (Table 2, Table S1).

CO_2 in the headspace increased rapidly in the beginning and then the increase slowed (Fig. 2). The initial rapid increase can be attributed to fast decomposition of the easily degradable substrates such as sugars, alcohols, etc. (Yang et al., 2016;Fey and Conrad, 2003;Glissmann and Conrad, 2002;Kotsyurbenko et al., 1993). As the easily degradable substrates were exhausted, the CO_2 production rate decreased. These observations are similar to those for the anaerobic incubations with

5 soils from a trough location in a high center polygon at the same site (Yang et al., 2016) and deep Siberian permafrost soils (Knoblauch et al., 2013). However, CO_2 continued to increase well beyond 2 months in both these previous studies , and the CO_2 production rates stabilized, probably reaching a rate limited by the slow rate of hydrolysis in the Siberian soil microcosms. These observations are different from the observed CO_2 level off in the current microcosms (Fig. 2a2, a4, a5).

10 CH_4 in the headspace increased slowly at the beginning and then accelerated (Fig. 2b1-5) except the center organic soils. CH_4 accumulation lagged behind CO_2 for about 10 d in most of the microcosms and by a few days for the center organic soil microcosms at 4 and 8 °C. These lag times are shorter than those observed in microcosms with deep Siberian permafrost soils (average 960 ± 300 d) (Knoblauch et al., 2013). This is probably because of the initial abundance of substrates such as organic acids in the Barrow soils (Fig. 2c1-6). In addition, the shallow Barrow soils experience freezing and thawing, and

15 microbial activity every year, while the deep Siberian permafrost soils were frozen for extended periods; as a result, the amount of initial biomass in the shallow Barrow soils is probably much higher than that in the deep Siberian soils.

Organic acids generally accumulated at the beginning, decreased as CH_4 concentration increased, and exhausted in the mineral soil microcosms (Fig. 2c1-6). In contrast, organic acids were not exhausted in the center organic soil microcosms

20 (Fig. 2c6). In comparison with similar tests with soils from the high center polygon trough, organic acids accumulated for over 5 months in the organic soils and were not exhausted in the mineral soils (Yang et al., 2016). The accumulation and disappearance of organic acids have been widely observed in the literature (van Bodegom and Stams, 1999;Fey et al., 2004;Glissmann and Conrad, 2002;Jerman et al., 2009;Kotsyurbenko et al., 1993;Lu et al., 2015;Peters and Conrad, 1996;Yao and Conrad, 1999).

Fe(II) concentrations increased and levelled off (Fig. 2d1-6), with similar trends for pH (Fig. 2e1-6). The pH increase concurred with Fe(III) reduction, which released hydroxides from Fe(OH)$_{3a}$ dissolution. The pH increase is in contrast to the observed pH decrease when Fe(III) reduction was absent (Xu et al., 2015). While Fe(III) reduction was reported to inhibit methanogenesis through direct inhibition (van Bodegom et al., 2004) or substrate competition (Miller et al., 2015;Reiche et

30 al., 2008), the impact appears less significant than expected in these incubations, as well as incubations with the high center polygon trough soils (Yang et al., 2016). This is consistent with the observation that methane production initiated in the presence of oxidants (Roy et al., 1997). In addition, Fe(III) reduction can both inhibit and promote methanogenesis (Zhuang et al., 2015). In the Barrow soils, the initial abundance of organic acids probably mitigates the competition between Fe(III) reducing and methanogenic populations, decreasing the lag time between CH_4 and CO_2 accumulation.

Substantial microbial activity was observed at -2 °C, which is above the soil water freezing point due to osmotic and matric potentials. These incubations led to an increase in CO_2 (Fig. 2a1-6), acetate (Fig. 2c1-6), Fe(II) (Fig. 2d1-6), and pH (Fig. 2e1-6). CH_4 concentrations were low but detectable in the headspace at -2 °C. The lag time between CH_4 and CO_2 increases

5   with decreasing temperature, which was widely observed in the literature as well (Fey and Conrad, 2003;Hoj et al., 2007;Jerman et al., 2009;van Bodegom and Scholten, 2001;Fey et al., 2004;Kotsyurbenko et al., 1993;Lu et al., 2015). The transition from -2 to 4 and 8 °C appears to be gradual except for the center organic soils, where CH_4 increases were drastic from -2 to 4 °C (Fig.2a1 vs. b1). The observed overall temperature responses are diverse, as manifested by Q_{10} values from 1.6 to 22 (Roy Chowdhury et al., 2015).

10   ### 3.2 Modeling results

3.2.1 Overall

With the same model parameter values given in Table 1 and Table S2 and different experimental parameter values listed in Table 2, the model roughly predicts the observed trends for different soils at the three temperatures (Fig. 2): CO_2 and CH_4 accumulate in the headspace; CO_2 accumulation slows down while CH_4 speeds up at later times; CH_4 lags behind CO_2;

15   organic acids accumulate and then decrease; Fe(II) accumulates and levels off; pH increases and levels off; and carbon mineralization and methanogenesis rates increase with temperature.

While the model predicts little CO_2 and CH_4 in the headspace at -2 °C, which is similar to what was observed, it predicts little change in Fe(II) and pH as well, which is not consistent with the observations. To improve the prediction at -2 °C,

20   which can be important (Zona et al., 2016;Xu et al., 2016a), it is necessary to understand why little CO_2 or CH_4 was observed to occur with Fe(III) reduction, which was indicated by the increase of Fe(II) and pH.

The same model parameter values describe the observed differences in the mineral soils better than in the organic soils. For the mineral soils, the model overpredicts the increasing trend for CO_2 in the headspace at late times because the observations

25   levelled off (Fig. 2a1-3). The initial rapid CO_2 increases lasted for over 2 months in the 3-year incubations with Siberian permafrost soils under 4 °C and anaerobic conditions (Knoblauch et al., 2013). In these long-term tests, CO_2 increased rapidly at the beginning and the rate stabilized as the carbon release became limited by hydrolysis of polymers. The observed sustained CO_2 accumulation in these closed microcosms indicates that the observed trends in Fig. 2a1-6 at later times are probably uncertain. Except for these mismatches, the model predictions generally agree with the observations for the mineral

30   soils reasonably well.

In contrast, the predictions do not agree as well with the observations for the organic soils. For the trough organic soils, the model underpredicts CO_2 in the headspace (Fig. 2a4) but describes the rest of the observations reasonably well. In addition to CO_2 (Fig. 2a5), the model underpredicts Fe(II) and pH increase in the ridge organic soils (Fig 2d5, e5). The prediction of the center organic soils differs from the observations the most (last column in Fig. 2). These mismatches might be explained by

5   model biases in initial Fe(III) content, LabileDOC, and biomasses.

3.2.2 Fe(III) reduction

Agreement between predictions and observations for the Fe(II) and pH increase can be improved for the ridge and center organic soils by increasing the Fe(III) content from f_{Fe3} = 0.005 to 0.01 and 0.02 (Fig. 2d5-6, e5-6). This also increases the predicted CO_2 and CH_4 for the center organic soils (Fig. 2a6, b6) because of the predicted pH increase (Fig. 2e6), which

10   increases the reaction rates as the pH response function increases when the calculated pH increases toward an optimal pH of 6.2 in Eq. (3). For the ridge organic soils, f_{Fe3} = 0.01 increases the predicted CH_4 like the center organic soils, but f_{Fe3} = 0.02 decreases CH_4 prediction because of the competition between methanogens and iron reducers and limited availability of substrates (Fig. 2b5). This provides an explanation as to why Fe(III) reduction can both supress and promote methanogenesis.

As the bioavailable Fe(III) in the organic soils is reported to range from 0.2 to 1 % of dry soil mass (Lipson et al., 2013a), the short-term tests are not expected to be Fe(III) limited for the mineral soils. Increasing bioavailable Fe(III) makes the model overpredict Fe(II) and pH increases at later times for the mineral soils (Fig. 2d1-5, e1-4), and Fe(III) reduction and methanogenesis at later times are predicted to be limited by organic substrate availability at 4 and 8 °C (Fig. 2b1-4). The

20   latter is consistent with the observed very low organic acids concentrations at the end (Fig. 2c1-5). As a result, the model underpredicts CH_4 accumulation, indicating the current parameterizations, in particular the half-saturation and growth rate constants, may over-predict the ability of iron reducing bacteria to outcompete methanogens.

3.2.3 CO_2 distribution among gas, aqueous, and adsorbed phases

While increasing Fe(III) slightly increases the predicted CO_2 for ridge mineral soils (Fig. 2a2), it decreases the predicted CO_2

25   in the headspace for trough and center mineral soils (Fig. 2a1 and a3). This is because CO_2 solubility is predicted to increase significantly as pH increases, resulting in the dissolution of CO_2 from the headspace into the aqueous phase (Fig. S1). To examine this impact, we conduct numerical simulations with a 45 mL headspace with an initial 1 atm N_2 gas and 10 mL solution with 10 mM total inorganic carbon at various temperature and pH values. $CO_2(g)$ and $CO_2(aq)$ or carbonic acid dominate at a pH lower than 5 (Fig. 3). As the pH increases above the carbonic acid pKa (around 6.3 at standard condition),

30   $CO_2(g)$ in the headspace and CO_2 in the aqueous phase decrease as HCO_3^- becomes dominant, and the gas-phase fraction decreases dramatically. The gas-phase fraction also decreases with decreasing temperatures (Fig. 3).

In addition, CO_2 was reported to adsorb to surface sites (Appelo et al., 2002;van Geen et al., 1994;Villalobos and Leckie, 2000). With the surface complexation reactions between $Fe(OH)_{3a}$ and carbonate species, we add 1 mmole $Fe(OH)_{3a}$ (about the mean values in Fig. 2 for the case $f_{Fe3} = 0.02$) to the abovementioned numerical experiments. The calculations show that the adsorption phase can dominate at low pH (Fig. S2), with the total amount dependent on the abundance of surface sites.

5   For the high-temperature high-Fe(III) initial content cases in Fig. 2, adding CO_2 sorption reactions provides a substantial buffer against the early increase in CO_2 in the headspace (Fig. S3). As the $Fe(OH)_{3a}$ is reduced and dissolved, the adsorbed CO_2 is predicted to be released, contributing to an increase in headspace CO_2 increase later on.

In addition to pressure, these calculations suggest the need to appropriately account for pH and its impact on the gas,
10   aqueous, and adsorbed phases CO_2 partition when we use headspace concentration measurements from anaerobic incubations to estimate CO_2 emission. Otherwise, substantial uncertainties can be introduced. A geochemical model with accurate thermodynamic data and accounting for CO_2 sorption can be useful in accurately quantifying CO_2 production in these closed microcosms.

3.2.4 Initial CO_2 accumulation in the organic soil microcosms

15   The model underpredicts the early CO_2 increase in the headspace for the organic soil microcosms (Fig. 2a4-6), which is mostly apparent in the center organic soil microcosms. The reason is that the organic soil microcosms contain more labile organic carbon than the mineral soil microcosms, as evidenced by WEOC (Table 2). In particular, the center organic soil microcosms contain about half the amount of TOTC of the other microcosms, double the water volume, and three to five times WEOC (Table 1). As a result, it produces the most CO_2 and CH_4 and has a very short lag time between CH_4 and CO_2.
20   If we increase the initial LabileDOC content $f_{labileDOC}$ from 0.0005, as shown in Fig. 2, to 0.01, and 0.02 for the organic soil microcosms, the model predicts an initial rapid CO_2 increase in the headspace that is comparable to that observed for trough and ridge microcosms but still less than that for the center organic soil microcosms (Fig. 4).

The predicted rapid initial CO_2 increase is due to the fast fermentation reactions (Fig. S4a1-6, e1-6). The predicted steep
25   transition in CO_2 concentration increases appears reasonable for the center and trough soil microcosms, but less so for the ridge soil microcosms. In addition to the 20 h and 14 d turnover time differences, fermentation reactions decrease the pH, further inhibit the predicted SOM1 decomposition reactions, Fe(III) reduction, and methanogenesis, making the predicted transition steeper. The fast fermentation is consistent with the observed rapid disappearance of glucose and increase of CO_2 after glucose addition in similar experiments with soils from a high center polygon trough from the same site (Yang et al.,
30   2016). However, the observed decrease of natural free reducing sugars is gradual, with about one-third of the original reducing sugars left over after 150 d of incubations. Along with the predicted rapid initial LabileDOC decrease and CO_2 increase, the model predicts a rapid initial increase in organic acids, which is close to the observations for the center soil microcosms but much greater than the observations for the trough and ridge soil microcosms. The latter indicates that the

ratio of organic acids to CO_2 of 2:1 from the fermentation reaction (R1) may not be accurately representative of the experiments.

5 Detailed measurements of organic acids showed a rapid initial increase and then a quick decrease of organic acids in the mineral soil microcosms and a gradual increase and slow decrease in the organic soil microcosms from the high center polygon trough near the site in the first 144 d anaerobic incubations (Yang et al., 2016). The rise and fall were fast in both the mineral and organic soil microcosms for ethanol, and were generally more gradual for organic acids than for ethanol (Yang et al., 2016). To explain the various observations for the organic soil microcosms and for accurate predictions, the diversity of the hydrolysis products (Feng and Simpson, 2008), and the subsequent pathways (Tveit et al., 2015) may need to
10 be accounted for. Additional detailed data are needed to support increasingly mechanistic models, e.g., with reducing sugars to represent less rapid fermentation, and additional specific organic acids such as propionate and butyrate to better describe diverse observations in the incubations.

3.2.5 Carbon mineralization

Less than about 1 % of the total initial carbon turned over to CO_2 and CH_4 in about 2 months, which is attributed mostly to
15 decomposition of SOM1, LabileDOC, and organic acids (Fig. S4). Few changes are predicted in the slow pools (SOM3, and SOM4, not shown) even though they comprise a large amount of carbon. The small amount of carbon turnover is similar to the incubation tests conducted with Siberian permafrost soils under 4 °C, which was estimated to be 3.1 % and 0.55 % under aerobic and anaerobic conditions for 1200 d (Knoblauch et al., 2013), the 1-year aerobic incubations tests (Feng and Simpson, 2008), and the incubations from a wide range of Arctic soils (Schädel et al., 2014). All of these results suggest that
20 the hydrolysis of macromolecular organics by extracellular enzymes is the rate-limiting step at late times. To predict the long-term vulnerability of the organic carbons, it is important to understand and describe the hydrolysis of macromolecular components in SOM.

3.2.6 CH_4 accumulation

Besides Fe(III) reduction, the predicted CH_4 production is dependent on the substrate production. With s_{labile} = 0.2, the model
25 generally predicts less CH_4 and more CO_2 than the case with s_{labile} = 0.4 because less SOM is assumed to respire through (or produce substrate for) the anaerobic pathway (Fig. S5). With increased s_{labile} = 0.6, the model predict more CH_4 and less CO_2. The impact on the mineral soils is generally more pronounced than the organic soils because the former is more substrate limiting than the latter. Unlike CO_2, CH_4 solubility and adsorption are much lower. Gas-phase CH_4 in the headspace dominates over aqueous and adsorbed phases. The model predicts the general exponential increase trend with a lag time
30 behind CO_2 (Fig. 2). However, the prediction is sensitive to Fe(III) reduction, pH, temperature (Fig. 2), and labile substrates (Fig. 4). The model substantially underpredicts early fast CH_4 production for the center organic soil microcosms. While the cell count for the center organic soils is not available for day 0, the data did show that the center organic soils had the highest

amount of biomass after 100 d incubations (Roy Chowdhury et al., 2015), indicating possible high initial abundance. The disagreement between the predictions and the observations can be mitigated by increasing the initial biomass f_{bio} from 10^{-6} to 10^{-5} and 2×10^{-5} for the center organic soil microcosms (Fig. 5). With increased initial biomass, Fe(III) reduction and methanogenesis are predicted to speed up the recovery of the initial pH drop caused by organic acids accumulation so that

5   the model predicts a fast CH_4 increase that is comparable to the observed. However, the model overpredicts the CH_4 increase at late times, indicating alternative inhibition mechanisms rather than substrate limitation on methanogenesis at late times or additional CH_4 consumption such as anaerobic oxidation (Caldwell et al., 2008;Smemo and Yavitt, 2011).

3.2.7 pH

With the complexation reactions involving proton or hydroxide anion with carbonate species, ferrihydrite surface, and SOM,

10   the geochemical model describes the observed pH evolution reasonably well (Fig. 2). The initial pH was lower in the mineral soils than in the organic soils (Fig. 2), probably because of less buffering capacity due to less organic matter in the mineral soils. Because the ridge mineral soils have the lowest initial pH, the CLM4Me pH factor is the lowest (Table S1), contributing to the underprediction of CH_4 (Fig. 2b2). With high organic content, the organic matter dominates the aqueous geochemistry, and the predicted pH is sensitive to the surface sites specified for WHAM. If the specified WHAM organic

15   matter is reduced by 25 %, then the pH buffer capacity is decreased and the predicted pH increases substantially (Fig. S6e1-6) even though the predicted changes in organic acids and Fe(II) are small. For the trough soils, the predicted pH surpasses the optimal of 6.2, and f(pH) decreases (Fig. S6e1, e4). As a result, predicted CO_2 and CH_4 are decreased. The pH impact becomes complex around the optimal pH. If we increase the specified WHAM organic matter by 25 %, the predicted pH is lower due to larger pH buffering and the reaction rates are generally smaller. Setting the WHAM sites at measured TOTC

20   works reasonably well for the experiments with the CLM4Me pH response function.

Comparing the CLM4Me pH response function with these used in TEM and DLEM, all three response functions show that the reaction rates are sensitive to pH (Fig. 6), which is expected to influence the predictions for these incubation tests as the pH increases from about 5.5 to 7. In this range, CLM4Me and DLEM have a similar slope, but the latter has a greater rate

25   reduction effect. While CLM4Me and TEM have a similar rate reduction effect, CLM4Me has a steeper curve than TEM. These differences translate to substantial differences in model predictions. All calculated f(pH) values increase during the tests (Fig. S7f1-f6). As the f(pH) calculated by DLEM is the lowest, the predicted changes are the smallest. The f(pH) calculated by TEM is slightly greater than CLM4Me at the beginning and is the opposite at late times (Fig. 6). As a result, TEM generally predicts slightly faster evolution than CLM4Me as the reaction rates at the late time are limited by substrates

30   rather than pH. While the pH ranges from 3.3 to 8.6 in the Arctic soils (Schädel et al., 2014), the range and the variability of the data are limited in the evaluation of these pH response functions. Nevertheless, model predictions are sensitive to pH response functions; the microbes are likely adapted to the site pH conditions such that the response functions are expected to

vary among sites and functional groups. Therefore, pH response function can be an important source of prediction uncertainty.

3.2.8 Temperature response

Temperature effects on reactions between inorganic aqueous species, and the aqueous and gas species, are taken into account in the established reaction database. The temperature impact on surface complexation reactions with ferric hydrous oxides, and with SOM in WHAM is not quantified, which can be a potential source of uncertainty. LSMs generally use empirical (e.g., CLM-CN, CENTURY), Q_{10}, or the Arrhenius equations. The CLM-CN temperature response function is compared with the CENTURY, Q_{10} equation, Arrhenius equation, and Ratkowsky equation in Fig. 7 and Fig. S8. All of these temperature response functions describe increasing rate with increasing temperature. When the temperature response functions $f(T)$ are plotted in arithmetical scale, the shapes are similar except for CENTURY, which approaches 1 when the temperature increases above 20 °C; CLM-CN is close to Q_{10} with $Q_{10} = 2.5$, the Arrhenius equation with $E_a = 60$ kJ mol^{-1} and the Ratkowsky equation with $T_m = 260$ K. When f(T) is plotted in log scale (Fig. 7), Q_{10} and Arrhenius equations are approximately linear while the rest have a similar shape; CLM-CN appears close to Ratkowsky equation with $T_m = 260$ K. At our temperatures -2, 4, and 8 °C, CLM-CN is very close to CENTURY, $Q_{10} = 2.5$, $E_a = 60$ kJ mol^{-1}, and $T_m = 260$ K (Fig. 7, Fig. S8). Despite their closeness, the predictions can be different for the different response functions (Fig. S9, Fig. S10), reflecting the sensitivity of the temperature effect on the biogeochemical reaction rates. The difference is amplified when different Q_{10}, E_a, or T_m is used (not shown), introducing potentially large uncertainty in model predictions. Because the temperature response functions are expected to vary for different micro-organisms, extra-cellular vs. intra-cellular enzymes, and geochemical reactions in the soil environment, improved quantification is needed.

4 Summary and conclusion

Soil organic carbon turnover and CO_2 and CH_4 production are sensitive to redox potential and pH. However, land surface models typically do not explicitly simulate the redox or pH, particularly in the aqueous phase, introducing uncertainty in greenhouse gas predictions. To account for the impact of availability of electron acceptors other than O_2 on soil organic matter (SOM) decomposition and methanogenesis, we extend the CLM-CN decomposition cascade to link complex polymers with simple substrates and add Fe(III) reduction and methanogenesis reactions. Because pH was observed to change substantially in the laboratory incubation tests and in the field and is a sensitive environmental variable for biogeochemical processes, we use the Windermere Humic Aqueous Model (WHAM) to simulate pH buffering by SOM. To account for the speciation of CO_2 among gas, aqueous, and solid (adsorbed) phases under varying pH, temperature, and pressure values, and the impact on typically measured headspace concentration, we use a geochemical model and an established reaction database to describe observations in recent anaerobic microcosms. Our results demonstrate the efficacy of using geochemical models to mechanistically represent the soil biogeochemical processes for Earth system models.

Together with the speciation reactions from the established geochemical database and surface complexation reactions for ferric hydrous oxides, WHAM enables us to approximately buffer an initial pH drop due to organic acid accumulation caused by fermentation and then a pH increase due to Fe(III) reduction and methanogenesis. The single input parameter for
5 WHAM is total organic carbon content, which is available in any SOM decomposition model. Therefore, adding WHAM does not necessitate any additional characterization. However, the temperature effects on surface complexation reactions with ferric hydrous oxides and organic matter may need to be further quantified.

The equilibrium geochemical speciation reactions predict a substantial increase in CO_2 solubility as the pH increases above
10 6.3 because the aqueous dominant species shifts from CO_2 to HCO_3^-. Adding CO_2 adsorption to surface sites of metal oxides further increases predicted solubility at low pH. Without taking into consideration of speciation, and pH, temperature and pressure impact with a geochemical model, the carbon mineralization rate can be substantially underestimated from anaerobic microcosms based on headspace CO_2 measurements.

15 Because different microbes respond to the temperature and pH change differently, it is challenging to describe observed diverse responses with any single one of the existing response functions. As the microbes adapt to the low temperature and pH conditions in the Arctic, the optimal growth temperature and pH value may need to be adjusted in these response functions.

20 We demonstrate that a geochemical model can mechanistically predict pH evolution and accounts for the impact of pH on biogeochemical reactions, which enhancing our understanding of and ability to quantify the experimental observations. Because pH is an important environmental variable in the ecosystems and land surface models either specify a fixed pH or use simple empirical equations, a geochemical model has the potential to improve model predictability for greenhouse emissions by mechanistically representing the soil biogeochemical processes.

25 **Code availability**

PHREEQC is publically available at http://wwwbrr.cr.usgs.gov/projects/GWC_coupled/phreeqc/.

Data availability

The experimental data, scripts to produce the PHREEQC input files, and plot the figures are archived at https://github.com/t6g/bgcs .

Appendix A Additional pH response functions

With pH_{min}, pH_{opt}, and pH_{max} of 4, 7 and 10 with no microbial activity at pH below pH_{min} or above pH_{max}, the pH response function used in DLEM is (Tian et al., 2010)

$$f(pH) = \frac{1.02}{1.02 + 10^6 \exp{(-2.5pH)}},$$

(A1)

5 for pH < 7; otherwise,

$$f(pH) = \frac{1.02}{1.02 + 10^6 \exp{(-2.5(14 - pH))}}.$$

(A2)

TEM uses a bell-shaped function (Cao et al., 1995;Xu et al., 2015;Raich et al., 1991)

$$f(pH) = \frac{(pH - pH_{min})(pH - pH_{max})}{(pH - pH_{min})(pH - pH_{max}) - (pH - pH_{opt})pH_{opt}},$$

(A3)

with pH_{min}, pH_{opt}, and pH_{max} = 5.5, 7.5, and 9, respectively (Cao et al., 1995). Considering the typical acidic conditions in

10 the Arctic and wetlands, we use the DLEM parameter values (Tian et al., 2010) as substantial CH_4 was observed in the incubation tests below pH 5.5 (Roy Chowdhury et al., 2015).

Appendix 2 Additional temperature response functions

The Q_{10} method is the most common temperature response function used in LSMs (Xu et al., 2016b;Berrittella and Van Huissteden, 2009, 2011;Walter and Heimann, 2000;Zhuang et al., 2004;Riley et al., 2011;Oleson et al., 2013). It is

15 $$f(T) = Q_{10}^{\frac{T - T_{ref}}{10}},$$

(B1)

with T_{ref} as a reference temperature usually at 25 °C. However, the Q_{10} value varies from 1.5 to 28 (Segers, 1998;Mikan et al., 2002), which indicates inadequate representation of the supply of substrates (Davidson and Janssens, 2006;Davidson et al., 2006), and microbial functional groups (Blake et al., 2015;Svensson, 1984;Rivkina et al., 2007;Lu et al., 2015) and necessitates alternative temperature response functions.

20 The Arrhenius equation (Arah and Stephen, 1998;Wang et al., 2012;Grant, 1998;Grant et al., 1993;Sharpe and DeMichele, 1977;Grant and Roulet, 2002) is

$$f(T) = \exp\left[-\frac{E_a}{R}\left(\frac{1}{T} - \frac{1}{T_{ref}}\right)\right],$$

(B2)

with E_a as the activation energy, and R as the gas constant. It is related to the Q_{10} method with $\ln(Q_{10}) = \frac{10E_a}{RT_{ref}T}$. The introduced variability by the absolute temperature T is not able to explain the wide range of Q_{10} values either. Consequently,

25 empirical equations are often used (Nicolardot et al., 1994). DayCent, ForCent, and CENTURY use (Parton et al., 2010)

$$f(T) = 0.56 + 0.465 atan[0.097(T - 15.7)].$$

(B3)

A temperature response function for microbial growth is (Ratkowsky et al., 1982)

$$f(T) = \left(\frac{T - T_m}{T_{ref} - T_m}\right)^2,$$

(B4)

with T_m as a conceptual temperature of no metabolic significance between 248-296 °K, depending on the bacterial cultures.

Acknowledgements

This research was funded by the U.S. Department of Energy, Office of Sciences, Biological and Environmental Research, Terrestrial Ecosystem Sciences Program, and is a product of the Next-Generation Ecosystem Experiments in the Arctic

5 (NGEE-Arctic) project. ORNL is managed by UT-Battelle, LLC, for the U.S. Department of Energy under contract DE-AC05-00OR22725.References

Disclaimer

This manuscript has been authored by UT-Battelle, LLC under contract no. DE-AC05-00OR22725 with the U.S. Department of Energy. The United States Government retains and the publisher, by accepting the article for publication, acknowledges

10 that the United States Government retains a non-exclusive, paid-up, irrevocable, worldwide license to publish or reproduce the published form of this manuscript, or allow others to do so, for United States Government purposes. The Department of Energy will provide public access to these results of federally sponsored research in accordance with the DOE Public Access Plan (http://energy.gov/downloads/doe-public-access-plan).

15 **References**

Abbott, B. W., Larouche, J. R., Jones, J. B., Bowden, W. B., and Balser, A. W.: Elevated dissolved organic carbon biodegradability from thawing and collapsing permafrost, Journal of Geophysical Research: Biogeosciences, 119, 2049-2063, 10.1002/2014JG002678, 2014.
Appelo, C. A. J., Van Der Weiden, M. J. J., Tournassat, C., and Charlet, L.: Surface Complexation of Ferrous Iron and Carbonate on Ferrihydrite and the Mobilization of Arsenic, Environmental Science & Technology, 36, 3096-3103, 10.1021/es010130n, 2002.
20 Arah, J. R. M., and Stephen, K. D.: A model of the processes leading to methane emission from peatland, Atmospheric Environment, 32, 3257-3264, 10.1016/S1352-2310(98)00052-1, 1998.
Arnosti, C.: Rapid potential rates of extracellular enzymatic hydrolysis in Arctic sediments, Limnology and Oceanography, 43, 315-324, 10.4319/lo.1998.43.2.0315, 1998.
Arnosti, C., Jørgensen, B. B., Sagemann, J., and Thamdrup, B.: Temperature dependence of microbial degradation of organic matter in
25 marine sediments: polysaccharide hydrolysis, oxygen consumption, and sulfate reduction, Marine Ecology-Progress Series, 165, 59-70, 10.3354/meps165059, 1998.
Arnosti, C.: Substrate specificity in polysaccharide hydrolysis: Contrasts between bottom water and sediments, Limnology and Oceanography, 45, 1112-1119, 10.4319/lo.2000.45.5.1112, 2000.
Berrittella, C., and Van Huissteden, J.: Uncertainties in modelling CH4 emissions from northern wetlands in glacial climates: effect of
30 hydrological model and CH4 model structure, Climate of the Past, 5, 361-373, 10.5194/cp-5-361-2009, 2009.
Berrittella, C., and van Huissteden, J.: Uncertainties in modelling CH4 emissions from northern wetlands in glacial climates: the role of vegetation parameters, Climate of the Past, 7, 1075-1087, 10.5194/cp-7-1075-2011, 2011.
Bethke, C. M., Sanford, R. A., Kirk, M. F., Jin, Q., and Flynn, T. M.: The thermodynamic ladder in geomicrobiology, Am J Sci, 311, 183-210, 10.2475/03.2011.01, 2011.
35 Blake, L. I., Tveit, A., Øvreås, L., Head, I. M., and Gray, N. D.: Response of Methanogens in Arctic Sediments to Temperature and Methanogenic Substrate Availability, PLoS ONE, 10, e0129733, 10.1371/journal.pone.0129733, 2015.
Bockheim, J. G., Hinkel, K. M., and Nelson, F. E.: Soils of the Barrow region, Alaska, Polar Geography, 25, 163-181, 10.1080/10889370109377711, 2001.
Bridgham, S. D., Cadillo-Quiroz, H., Keller, J. K., and Zhuang, Q.: Methane emissions from wetlands: biogeochemical, microbial, and
40 modeling perspectives from local to global scales, Global Change Biology, 19, 1325-1346, 10.1111/gcb.12131, 2013.

Caldwell, S. L., Laidler, J. R., Brewer, E. A., Eberly, J. O., Sandborgh, S. C., and Colwell, F. S.: Anaerobic Oxidation of Methane: Mechanisms, Bioenergetics, and the Ecology of Associated Microorganisms, Environmental Science & Technology, 42, 6791-6799, 10.1021/es800120b, 2008.

Cao, M., Dent, J. B., and Heal, O. W.: Modeling methane emissions from rice paddies, Global Biogeochemical Cycles, 9, 183-195, 10.1029/94GB03231, 1995.

Cao, M., Gregson, K., and Marshall, S.: Global methane emission from wetlands and its sensitivity to climate change, Atmospheric Environment, 32, 3293-3299, 10.1016/S1352-2310(98)00105-8, 1998.

Cheng, K., Ogle, S. M., Parton, W. J., and Pan, G.: Predicting methanogenesis from rice paddies using the DAYCENT ecosystem model, Ecological Modelling, 261–262, 19-31, 10.1016/j.ecolmodel.2013.04.003, 2013.

Conrad, R.: Soil microorganisms as controllers of atmospheric trace gases (H2, CO, CH4, OCS, N2O, and NO), Microbiological Reviews, 60, 609-640, 1996.

Cui, M., Ma, A., Qi, H., Zhuang, X., Zhuang, G., and Zhao, G.: Warmer temperature accelerates methane emissions from the Zoige wetland on the Tibetan Plateau without changing methanogenic community composition, Scientific Reports, 5, 11616, 10.1038/srep11616, 2015.

Davidson, E. A., and Janssens, I. A.: Temperature sensitivity of soil carbon decomposition and feedbacks to climate change, Nature, 440, 165-173, 2006.

Davidson, E. A., Janssens, I. A., and Luo, Y.: On the variability of respiration in terrestrial ecosystems: moving beyond Q10, Global Change Biology, 12, 154-164, 10.1111/j.1365-2486.2005.01065.x, 2006.

Drake, H. L., Horn, M. A., and Wüst, P. K.: Intermediary ecosystem metabolism as a main driver of methanogenesis in acidic wetland soil, Environmental Microbiology Reports, 1, 307-318, 10.1111/j.1758-2229.2009.00050.x, 2009.

Drake, T. W., Wickland, K. P., Spencer, R. G. M., McKnight, D. M., and Striegl, R. G.: Ancient low–molecular-weight organic acids in permafrost fuel rapid carbon dioxide production upon thaw, Proceedings of the National Academy of Sciences, 2015.

Dunfield, P., knowles, R., Dumont, R., and Moore, T. R.: Methane production and consumption in temperate and subarctic peat soils: Response to temperature and pH, Soil Biology and Biochemistry, 25, 321-326, 10.1016/0038-0717(93)90130-4, 1993.

Dzombak, D. A., and Morel, F.: Surface complexation modeling: hydrous ferric oxide, Wiley, 1990.

Elberling, B., Michelsen, A., Schadel, C., Schuur, E. A. G., Christiansen, H. H., Berg, L., Tamstorf, M. P., and Sigsgaard, C.: Long-term CO2 production following permafrost thaw, Nature Clim. Change, 3, 890-894, 10.1038/nclimate1955, 2013.

Estop-Aragonés, C., and Blodau, C.: Effects of experimental drying intensity and duration on respiration and methane production recovery in fen peat incubations, Soil Biology and Biochemistry, 47, 1-9, 10.1016/j.soilbio.2011.12.008, 2012.

Feng, X., and Simpson, M. J.: Temperature responses of individual soil organic matter components, Journal of Geophysical Research: Biogeosciences, 113, n/a-n/a, 10.1029/2008JG000743, 2008.

Fey, A., and Conrad, R.: Effect of temperature on the rate limiting step in the methanogenic degradation pathway in rice field soil, Soil Biology and Biochemistry, 35, 1-8, 10.1016/S0038-0717(02)00175-X, 2003.

Fey, A., Claus, P., and Conrad, R.: Temporal change of 13C-isotope signatures and methanogenic pathways in rice field soil incubated anoxically at different temperatures, Geochimica et Cosmochimica Acta, 68, 293-306, 10.1016/S0016-7037(03)00426-5, 2004.

Forster, P., Ramaswamy, V., Artaxo, P., Berntsen, T., Betts, R., Fahey, D. W., Haywood, J., Lean, J., Lowe, D. C., and Myhre, G.: Changes in atmospheric constituents and in radiative forcing. Chapter 2, in: Climate Change 2007. The Physical Science Basis, 2007.

Fumoto, T., Kobayashi, K., Li, C., Yagi, K., and Hasegawa, T.: Revising a process-based biogeochemistry model (DNDC) to simulate methane emission from rice paddy fields under various residue management and fertilizer regimes, Global Change Biology, 14, 382-402, 10.1111/j.1365-2486.2007.01475.x, 2008.

Garcia, J.-L., Patel, B. K. C., and Ollivier, B.: Taxonomic, Phylogenetic, and Ecological Diversity of Methanogenic Archaea, Anaerobe, 6, 205-226, 10.1006/anae.2000.0345, 2000.

Glissmann, K., and Conrad, R.: Saccharolytic activity and its role as a limiting step in methane formation during the anaerobic degradation of rice straw in rice paddy soil, Biol Fertil Soils, 35, 62-67, 10.1007/s00374-002-0442-z, 2002.

Grant, R. F., Juma, N. G., and McGill, W. B.: Simulation of carbon and nitrogen transformations in soil: Mineralization, Soil Biology and Biochemistry, 25, 1317-1329, 10.1016/0038-0717(93)90046-E, 1993.

Grant, R. F.: Simulation of methanogenesis in the mathematical model ecosys, Soil Biology and Biochemistry, 30, 883-896, 10.1016/S0038-0717(97)00218-6, 1998.

Grant, R. F., and Roulet, N. T.: Methane efflux from boreal wetlands: Theory and testing of the ecosystem model Ecosys with chamber and tower flux measurements, Global Biogeochemical Cycles, 16, 1054, 10.1029/2001gb001702, 2002.

Hao, L.-P., Lü, F., Li, L., Shao, L.-M., and He, P.-J.: Shift of pathways during initiation of thermophilic methanogenesis at different initial pH, Bioresource Technology, 126, 418-424, 10.1016/j.biortech.2011.12.072, 2012.

Herndon, E. M., Mann, B. F., Chowdhury, T. R., Yang, Z., Wullschleger, S. D., Graham, D., Liang, L., and Gu, B.: Pathways of anaerobic organic matter decomposition in tundra soils from Barrow, Alaska, Journal of Geophysical Research: Biogeosciences, n/a-n/a, 10.1002/2015JG003147, 2015a.

Herndon, E. M., Yang, Z., Bargar, J., Janot, N., Regier, T. Z., Graham, D. E., Wullschleger, S. D., Gu, B., and Liang, L.: Geochemical drivers of organic matter decomposition in arctic tundra soils, Biogeochemistry, 126, 397-414, 10.1007/s10533-015-0165-5, 2015b.

Hodgkins, S. B., Tfaily, M. M., McCalley, C. K., Logan, T. A., Crill, P. M., Saleska, S. R., Rich, V. I., and Chanton, J. P.: Changes in peat chemistry associated with permafrost thaw increase greenhouse gas production, Proceedings of the National Academy of Sciences of the United States of America, 111, 5819-5824, 10.1073/pnas.1314641111, 2014.

Hoj, L., Olsen, R. A., and Torsvik, V. L.: Effects of temperature on the diversity and community structure of known methanogenic groups and other archaea in high Arctic peat, ISME J, 2, 37-48, 2007.

IPCC: Climate Change 2013: The Physical Science Basis. Contribution of Working Group I to the Fifth Assessment Report of the Intergovernmental Panel on Climate Change, Cambridge University Press, Cambridge, United Kingdom and New York, NY, USA, 1535 pp., 2013.

Istok, J. D., Park, M., Michalsen, M., Spain, A. M., Krumholz, L. R., Liu, C., McKinley, J., Long, P., Roden, E., Peacock, A. D., and Baldwin, B.: A thermodynamically-based model for predicting microbial growth and community composition coupled to system geochemistry: Application to uranium bioreduction, Journal of Contaminant Hydrology, 112, 1-14, 10.1016/j.jconhyd.2009.07.004, 2010.

Jerman, V., Metje, M., Mandić-Mulec, I., and Frenzel, P.: Wetland restoration and methanogenesis: the activity of microbial populations and competition for substrates at different temperatures, Biogeosciences, 6, 1127-1138, 10.5194/bg-6-1127-2009, 2009.

Jin, Q., and Roden, E. E.: Microbial physiology-based model of ethanol metabolism in subsurface sediments, Journal of Contaminant Hydrology, 125, 1-12, 10.1016/j.jconhyd.2011.04.002, 2011.

Kettunen, A.: Connecting methane fluxes to vegetation cover and water table fluctuations at microsite level: A modeling study, Global Biogeochemical Cycles, 17, n/a-n/a, 10.1029/2002GB001958, 2003.

Knoblauch, C., Beer, C., Sosnin, A., Wagner, D., and Pfeiffer, E.-M.: Predicting long-term carbon mineralization and trace gas production from thawing permafrost of Northeast Siberia, Global Change Biology, 19, 1160-1172, 10.1111/gcb.12116, 2013.

Knorr, K.-H., and Blodau, C.: Impact of experimental drought and rewetting on redox transformations and methanogenesis in mesocosms of a northern fen soil, Soil Biology and Biochemistry, 41, 1187-1198, 10.1016/j.soilbio.2009.02.030, 2009.

Kögel-Knabner, I.: The macromolecular organic composition of plant and microbial residues as inputs to soil organic matter, Soil Biology and Biochemistry, 34, 139-162, 10.1016/S0038-0717(01)00158-4, 2002.

Kotsyurbenko, O. R., Nozhevnikova, A. N., and Zavarzin, G. A.: Methanogenic degradation of organic matter by anaerobic bacteria at low temperature, Chemosphere, 27, 1745-1761, 10.1016/0045-6535(93)90155-X, 1993.

Kotsyurbenko, O. R., Chin, K.-J., Glagolev, M. V., Stubner, S., Simankova, M. V., Nozhevnikova, A. N., and Conrad, R.: Acetoclastic and hydrogenotrophic methane production and methanogenic populations in an acidic West-Siberian peat bog, Environmental Microbiology, 6, 1159-1173, 10.1111/j.1462-2920.2004.00634.x, 2004.

Kotsyurbenko, O. R., Friedrich, M. W., Simankova, M. V., Nozhevnikova, A. N., Golyshin, P. N., Timmis, K. N., and Conrad, R.: Shift from Acetoclastic to H2-Dependent Methanogenesis in a West Siberian Peat Bog at Low pH Values and Isolation of an Acidophilic Methanobacterium Strain, Applied and Environmental Microbiology, 73, 2344-2348, 2007.

Koven, C. D., Schuur, E. A. G., Schädel, C., Bohn, T. J., Burke, E. J., Chen, G., Chen, X., Ciais, P., Grosse, G., Harden, J. W., Hayes, D. J., Hugelius, G., Jafarov, E. E., Krinner, G., Kuhry, P., Lawrence, D. M., MacDougall, A. H., Marchenko, S. S., McGuire, A. D., Natali, S. M., Nicolsky, D. J., Olefeldt, D., Peng, S., Romanovsky, V. E., Schaefer, K. M., Strauss, J., Treat, C. C., and Turetsky, M.: A simplified, data-consrained approach to estimate the permafrost carbon–climate feedback, Philosophical Transactions of the Royal Society of London A: Mathematical, Physical and Engineering Sciences, 373, 2015.

Lavoie, M., Mack, M. C., and Schuur, E. A. G.: Effects of elevated nitrogen and temperature on carbon and nitrogen dynamics in Alaskan arctic and boreal soils, Journal of Geophysical Research: Biogeosciences, 116, n/a-n/a, 10.1029/2010JG001629, 2011.

Lee, H., Schuur, E. A. G., Inglett, K. S., Lavoie, M., and Chanton, J. P.: The rate of permafrost carbon release under aerobic and anaerobic conditions and its potential effects on climate, Global Change Biology, 18, 515-527, 10.1111/j.1365-2486.2011.02519.x, 2012.

Lipson, D. A., Jha, M., Raab, T. K., and Oechel, W. C.: Reduction of iron (III) and humic substances plays a major role in anaerobic respiration in an Arctic peat soil, Journal of Geophysical Research: Biogeosciences, 115, n/a-n/a, 10.1029/2009JG001147, 2010.

Lipson, D. A., Haggerty, J. M., Srinivas, A., Raab, T. K., Sathe, S., and Dinsdale, E. A.: Metagenomic Insights into Anaerobic Metabolism along an Arctic Peat Soil Profile, PLoS ONE, 8, e64659, 10.1371/journal.pone.0064659, 2013a.

Lipson, D. A., Raab, T. K., Goria, D., and Zlamal, J.: The contribution of Fe(III) and humic acid reduction to ecosystem respiration in drained thaw lake basins of the Arctic Coastal Plain, Global Biogeochemical Cycles, 27, 399-409, 10.1002/gbc.20038, 2013b.

Lloyd, J., and Taylor, J. A.: On the Temperature Dependence of Soil Respiration, Functional Ecology, 8, 315-323, 1994.

Lu, Y., Fu, L., Lu, Y., Hugenholtz, F., and Ma, K.: Effect of temperature on the structure and activity of a methanogenic archaeal community during rice straw decomposition, Soil Biology and Biochemistry, 81, 17-27, 10.1016/j.soilbio.2014.10.031, 2015.

Madigan, M. T.: Brock biology of microorganisms, Benjamin Cummings, San Francisco, 2012.

Mann, B. F., Chen, H., Herndon, E. M., Chu, R. K., Tolic, N., Portier, E. F., Roy Chowdhury, T., Robinson, E. W., Callister, S. J., Wullschleger, S. D., Graham, D. E., Liang, L., and Gu, B.: Indexing Permafrost Soil Organic Matter Degradation Using High-Resolution Mass Spectrometry, PLoS ONE, 10, e0130557, 10.1371/journal.pone.0130557, 2015.

Manzoni, S., and Porporato, A.: Soil carbon and nitrogen mineralization: Theory and models across scales, Soil Biology and Biochemistry, 41, 1355-1379, 10.1016/j.soilbio.2009.02.031, 2009.

Mikan, C. J., Schimel, J. P., and Doyle, A. P.: Temperature controls of microbial respiration in arctic tundra soils above and below freezing, Soil Biology and Biochemistry, 34, 1785-1795, 10.1016/S0038-0717(02)00168-2, 2002.

Miller, K. E., Lai, C.-T., Friedman, E. S., Angenent, L. T., and Lipson, D. A.: Methane suppression by iron and humic acids in soils of the Arctic Coastal Plain, Soil Biology and Biochemistry, 83, 176-183, 10.1016/j.soilbio.2015.01.022, 2015.

Nicolardot, B., Fauvet, G., and Cheneby, D.: Carbon and nitrogen cycling through soil microbial biomass at various temperatures, Soil Biology and Biochemistry, 26, 253-261, 10.1016/0038-0717(94)90165-1, 1994.

Oleson, K., Lawrence, D., Bonan, G., Levis, S., Swenson, S., Thornton, P., Bozbiyik, A., Fisher, R., Heald, C., Kluzek, E., Lamarque, J.-F., Lawrence, P., Lipscomb, W., Muszala, S., and Sacks, W.: Technical description of version 4.5 of the Community Land Model (CLM), NCAR, 2013.

Parkhurst, D. L., and Appelo, C.: Description of input and examples for PHREEQC version 3: a computer program for speciation, batch-reaction, one-dimensional transport, and inverse geochemical calculations, US Geological Survey2328-7055, 2013.

Parton, W. J., Hanson, P. J., Swanston, C., Torn, M., Trumbore, S. E., Riley, W., and Kelly, R.: ForCent model development and testing using the Enriched Background Isotope Study experiment, J. Geophys. Res., 115, G04001, 10.1029/2009jg001193, 2010.

Peters, V., and Conrad, R.: Sequential reduction processes and initiation of CH4 production upon flooding of oxic upland soils, Soil Biology and Biochemistry, 28, 371-382, 10.1016/0038-0717(95)00146-8, 1996.

Raich, J. W., Rastetter, E. B., Melillo, J. M., Kicklighter, D. W., Steudler, P. A., Peterson, B. J., Grace, A. L., Moore Iii, B., and Vorosmarty, C. J.: Potential net primary productivity in South America: application of a global model, Ecological Applications, 1, 399-429, 10.2307/1941899, 1991.

Ratkowsky, D. A., Olley, J., McMeekin, T. A., and Ball, A.: Relationship between temperature and growth rate of bacterial cultures, Journal of Bacteriology, 149, 1-5, 1982.

Reiche, M., Torburg, G., and Küsel, K.: Competition of Fe(III) reduction and methanogenesis in an acidic fen, FEMS Microbiology Ecology, 65, 88-101, 2008.

Riley, W. J., Subin, Z. M., Lawrence, D. M., Swenson, S. C., Torn, M. S., Meng, L., Mahowald, N. M., and Hess, P.: Barriers to predicting changes in global terrestrial methane fluxes: analyses using CLM4Me, a methane biogeochemistry model integrated in CESM, Biogeosciences, 8, 1925-1953, 10.5194/bg-8-1925-2011, 2011.

Riley, W. J., Maggi, F., Kleber, M., Torn, M. S., Tang, J. Y., Dwivedi, D., and Guerry, N.: Long residence times of rapidly decomposable soil organic matter: application of a multi-phase, multi-component, and vertically resolved model (BAMS1) to soil carbon dynamics, Geosci. Model Dev., 7, 1335-1355, 10.5194/gmd-7-1335-2014, 2014.

Rittmann, B. E., and McCarty, P. L.: Environmental biotechnology: principles and applications, McGraw-Hill, 2001.

Rivkina, E., Shcherbakova, V., Laurinavichius, K., Petrovskaya, L., Krivushin, K., Kraev, G., Pecheritsina, S., and Gilichinsky, D.: Biogeochemistry of methane and methanogenic archaea in permafrost, FEMS Microbiology Ecology, 61, 1-15, 2007.

Roy Chowdhury, T., Herndon, E. M., Phelps, T. J., Elias, D. A., Gu, B., Liang, L., Wullschleger, S. D., and Graham, D. E.: Stoichiometry and temperature sensitivity of methanogenesis and CO2 production from saturated polygonal tundra in Barrow, Alaska, Global Change Biology, 21, 722-737, 10.1111/gcb.12762, 2015.

Roy, R., Klüber, H. D., and Conrad, R.: Early initiation of methane production in anoxic rice soil despite the presence of oxidants, FEMS Microbiology Ecology, 24, 311-320, 10.1016/S0168-6496(97)00072-X, 1997.

Schädel, C., Schuur, E. A. G., Bracho, R., Elberling, B., Knoblauch, C., Lee, H., Luo, Y., Shaver, G. R., and Turetsky, M. R.: Circumpolar assessment of permafrost C quality and its vulnerability over time using long-term incubation data, Global Change Biology, 20, 641-652, 10.1111/gcb.12417, 2014.

Schädel, C., Bader, M., Schuur, E. A., Bracho, R., Capek, P., De-Baets, S., Diakova, K., Ernakovich, J., Estop-Aragones, C., Graham, D. E., Hartley, I. P., Iversen, C. M., Kane, E., Knoblauch, C., Lupascu, M., Natali, S., Norby, R. J., O'Donnell, J. A., Roy Chowdhury, T., Šantrůčková, H., Shaver, G., Sloan, V. L., Treat, C. C., Turetsky, M. R., Waldrop, M., and Wickland, K. P.: Potential carbon emissions dominated by carbon dioxide from thawed permafrost soils, . Nature Climate Change, in press, 2016.

Segers, R.: Methane production and methane consumption: a review of processes underlying wetland methane fluxes, Biogeochemistry, 41, 23-51, 10.1023/A:1005929032764, 1998.

Segers, R., and Kengen, S. W. M.: Methane production as a function of anaerobic carbon mineralization: A process model, Soil Biology and Biochemistry, 30, 1107-1117, 10.1016/S0038-0717(97)00198-3, 1998.

Sharpe, P. J. H., and DeMichele, D. W.: Reaction kinetics of poikilotherm development, Journal of Theoretical Biology, 64, 649-670, 10.1016/0022-5193(77)90265-X, 1977.

Smemo, K. A., and Yavitt, J. B.: Anaerobic oxidation of methane: an underappreciated aspect of methane cycling in peatland ecosystems?, Biogeosciences, 8, 779-793, 10.5194/bg-8-779-2011, 2011.

Sowers, K. R., Baron, S. F., and Ferry, J. G.: Methanosarcina-Acetivorans Sp-Nov, An Acetotrophic Methane-Producing Bacterium Isolated from Marine-Sediments, Applied and Environmental Microbiology, 47, 971-978, 1984.

Svensson, B. H.: Different Temperature Optima for Methane Formation When Enrichments from Acid Peat Are Supplemented with Acetate or Hydrogen, Applied and Environmental Microbiology, 48, 389-394, 1984.

Tang, G., Luo, W., Watson, D. B., Brooks, S. C., and Gu, B.: Prediction of Aluminum, Uranium, and Co-Contaminants Precipitation and Adsorption during Titration of Acidic Sediments, Environmental Science & Technology, 47, 5787-5793, 10.1021/es400169y, 2013a.

Tang, G., Watson, D. B., Wu, W.-M., Schadt, C. W., Parker, J. C., and Brooks, S. C.: U(VI) Bioreduction with Emulsified Vegetable Oil as the Electron Donor – Model Application to a Field Test, Environmental Science & Technology, 47, 3218-3225, 10.1021/es304643h, 2013b.

Tang, G., Wu, W.-M., Watson, D. B., Parker, J. C., Schadt, C. W., Shi, X., and Brooks, S. C.: U(VI) Bioreduction with Emulsified Vegetable Oil as the Electron Donor – Microcosm Tests and Model Development, Environmental Science & Technology, 47, 3209-3217, 10.1021/es304641b, 2013c.

Tang, G., Yuan, F., Bisht, G., Hammond, G. E., Lichtner, P. C., Kumar, J., Mills, R. T., Xu, X., Andre, B., Hoffman, F. M., Painter, S. L., and Thornton, P. E.: Addressing numerical challenges in introducing a reactive transport code into a land surface model: a biogeochemical modeling proof-of-concept with CLM–PFLOTRAN 1.0, Geosci. Model Dev., 9, 927-946, 10.5194/gmd-9-927-2016, 2016.

Thornton, P. E., and Rosenbloom, N. A.: Ecosystem model spin-up: Estimating steady state conditions in a coupled terrestrial carbon and nitrogen cycle model, Ecological Modelling, 189, 25-48, 10.1016/j.ecolmodel.2005.04.008, 2005.

Tian, H., Xu, X., Liu, M., Ren, W., Zhang, C., Chen, G., and Lu, C.: Spatial and temporal patterns of CH4 and N2O fluxes in terrestrial ecosystems of North America during 1979–2008: application of a global biogeochemistry model, Biogeosciences, 7, 2673-2694, 10.5194/bg-7-2673-2010, 2010.

Tian, H., Chen, G., Lu, C., Xu, X., Ren, W., Zhang, B., Banger, K., Tao, B., Pan, S., Liu, M., Zhang, C., Bruhwiler, L., and Wofsy, S.: Global methane and nitrous oxide emissions from terrestrial ecosystems due to multiple environmental changes, Ecosystem Health and Sustainability, 1, 1-20, 10.1890/EHS14-0015.1, 2015.

Tipping, E.: WHAM—A chemical equilibrium model and computer code for waters, sediments, and soils incorporating a discrete site/electrostatic model of ion-binding by humic substances, Computers & Geosciences, 20, 973-1023, 10.1016/0098-3004(94)90038-8, 1994.

Treat, C. C., Natali, S. M., Ernakovich, J., Iversen, C. M., Lupascu, M., McGuire, A. D., Norby, R. J., Roy Chowdhury, T., Richter, A., Šantrůčková, H., Schädel, C., Schuur, E. A. G., Sloan, V. L., Turetsky, M. R., and Waldrop, M. P.: A pan-Arctic synthesis of CH4 and CO2 production from anoxic soil incubations, Global Change Biology, 21, 2787-2803, 10.1111/gcb.12875, 2015.

Tveit, A., Schwacke, R., Svenning, M. M., and Urich, T.: Organic carbon transformations in high-Arctic peat soils: key functions and microorganisms, The ISME Journal, 7, 299-311, 10.1038/ismej.2012.99, 2013.

Tveit, A. T., Urich, T., Frenzel, P., and Svenning, M. M.: Metabolic and trophic interactions modulate methane production by Arctic peat microbiota in response to warming, Proceedings of the National Academy of Sciences of the United States of America, 112, E2507-E2516, 10.1073/pnas.1420797112, 2015.

Van Bodegom, P., Goudriaan, J., and Leffelaar, P.: A mechanistic model on methane oxidation in a rice rhizosphere, Biogeochemistry, 55, 145-177, 10.1023/a:1010640515283, 2001.

van Bodegom, P. M., and Stams, A. J. M.: Effects of alternative electron acceptors and temperature on methanogenesis in rice paddy soils, Chemosphere, 39, 167-182, 10.1016/S0045-6535(99)00101-0, 1999.

van Bodegom, P. M., Leffelaar, P. A., Stams, A. J. M., and Wassmann, R.: Modeling methane emissions from rice fields: Variability, uncertainty, and sensitivity analysis of processes involved, Nutrient Cycling in Agroecosystems, 58, 231-248, 10.1023/a:1009854905333, 2000.

van Bodegom, P. M., and Scholten, J. C. M.: Microbial processes of CH4 production in a rice paddy soil: model and experimental validation, Geochimica et Cosmochimica Acta, 65, 2055-2066, 10.1016/S0016-7037(01)00563-4, 2001.

van Bodegom, P. M., Scholten, J. C. M., and Stams, A. J. M.: Direct inhibition of methanogenesis by ferric iron, FEMS Microbiology Ecology, 49, 261-268, 10.1016/j.femsec.2004.03.017, 2004.

van Geen, A., Robertson, A. P., and Leckie, J. O.: Complexation of carbonate species at the goethite surface: Implications for adsorption of metal ions in natural waters, Geochimica et Cosmochimica Acta, 58, 2073-2086, 10.1016/0016-7037(94)90286-0, 1994.

Van Kessel, J. A. S., and Russell, J. B.: The effect of pH on ruminal methanogenesis, FEMS Microbiology Ecology, 20, 205-210, 10.1016/0168-6496(96)00030-X, 1996.

Villalobos, M., and Leckie, J. O.: Carbonate adsorption on goethite under closed and open CO2 conditions, Geochimica et Cosmochimica Acta, 64, 3787-3802, 10.1016/S0016-7037(00)00465-8, 2000.

Walter, B. P., and Heimann, M.: A process-based, climate-sensitive model to derive methane emissions from natural wetlands: Application to five wetland sites, sensitivity to model parameters, and climate, Global Biogeochemical Cycles, 14, 745-765, 10.1029/1999gb001204, 2000.

Wang, G., Post, W. M., and Mayes, M. A.: Development of microbial-enzyme-mediated decomposition model parameters through steady-state and dynamic analyses, Ecological Applications, 23, 255-272, 10.1890/12-0681.1, 2012.

Wang, Z. P., DeLaune, R. D., Patrick, W. H., and Masscheleyn, P. H.: Soil Redox and pH Effects on Methane Production in a Flooded Rice Soil, Soil Science Society of America Journal, 57, 10.2136/sssaj1993.03615995005700020016x, 1993.

Wania, R., Ross, I., and Prentice, I. C.: Implementation and evaluation of a new methane model within a dynamic global vegetation model: LPJ-WHyMe v1.3.1, Geosci. Model Dev., 3, 565-584, 10.5194/gmd-3-565-2010, 2010.

Wania, R., Melton, J. R., Hodson, E. L., Poulter, B., Ringeval, B., Spahni, R., Bohn, T., Avis, C. A., Chen, G., Eliseev, A. V., Hopcroft, P. O., Riley, W. J., Subin, Z. M., Tian, H., van Bodegom, P. M., Kleinen, T., Yu, Z. C., Singarayer, J. S., Zurcher, S., Lettenmaier, D. P.,

5 Beerling, D. J., Denisov, S. N., Prigent, C., Papa, F., and Kaplan, J. O.: Present state of global wetland extent and wetland methane modelling: methodology of a model inter-comparison project (WETCHIMP), Geoscientific Model Development, 6, 617-641, 10.5194/gmd-6-617-2013, 2013.

Weedon, J. T., Aerts, R., Kowalchuk, G. A., van Logtestijn, R., Andringa, D., and van Bodegom, P. M.: Temperature sensitivity of peatland C and N cycling: Does substrate supply play a role?, Soil Biology & Biochemistry, 61, 109-120, 10.1016/j.soilbio.2013.02.019,

10 2013.

Xu, X., and Tian, H.: Methane exchange between marshland and the atmosphere over China during 1949–2008, Global Biogeochemical Cycles, 26, GB2006, 10.1029/2010GB003946, 2012.

Xu, X., Elias, D. A., Graham, D. E., Phelps, T. J., Carroll, S. L., Wullschleger, S. D., and Thornton, P. E.: A microbial functional group-based module for simulating methane production and consumption: Application to an incubated permafrost soil, Journal of Geophysical

15 Research: Biogeosciences, 120, 1315-1333, 10.1002/2015JG002935, 2015.

Xu, X., Riley, W. J., Koven, C. D., Billesbach, D. P., Chang, R. Y. W., Commane, R., Euskirchen, E. S., Hartery, S., Harazono, Y., Iwata, H., McDonald, K. C., Miller, C. E., Oechel, W. C., Poulter, B., Raz-Yaseef, N., Sweeney, C., Torn, M., Wofsy, S. C., Zhang, Z., and Zona, D.: A multi-scale comparison of modeled and observed seasonal methane cycles in northern wetlands, Biogeosciences Discuss., 2016, 1-30, 10.5194/bg-2016-167, 2016a.

20 Xu, X., Yuan, F., Hanson, P. J., Wullschleger, S. D., Thornton, P. E., Riley, W. J., Song, X., Graham, D. E., Song, C., and Tian, H.: Reviews and syntheses: Four Decades of Modeling Methane Cycling in Terrestrial Ecosystems, Biogeosciences Discuss., 2016, 1-56, 10.5194/bg-2016-37, 2016b.

Yang, Z., Wullschleger, S. D., Liang, L., Graham, D. E., and Gu, B.: Effects of warming on the degradation and production of low-molecular-weight labile organic carbon in an Arctic tundra soil, Soil Biology and Biochemistry, 95, 202-211,

25 10.1016/j.soilbio.2015.12.022, 2016.

Yao, H., and Conrad, R.: Thermodynamics of methane production in different rice paddy soils from China, the Philippines and Italy, Soil Biology and Biochemistry, 31, 463-473, 10.1016/S0038-0717(98)00152-7, 1999.

Yao, H., Conrad, R., Wassmann, R., and Neue, H. U.: Effect of soil characteristics on sequential reduction and methane production in sixteen rice paddy soils from China, the Philippines, and Italy, Biogeochemistry, 47, 269-295, 10.1007/BF00992910, 1999.

30 Zhuang, L., Xu, J., Tang, J., and Zhou, S.: Effect of ferrihydrite biomineralization on methanogenesis in an anaerobic incubation from paddy soil, Journal of Geophysical Research: Biogeosciences, 120, 876-886, 10.1002/2014JG002893, 2015.

Zhuang, Q., Melillo, J. M., Kicklighter, D. W., Prinn, R. G., McGuire, A. D., Steudler, P. A., Felzer, B. S., and Hu, S.: Methane fluxes between terrestrial ecosystems and the atmosphere at northern high latitudes during the past century: A retrospective analysis with a process-based biogeochemistry model, Global Biogeochemical Cycles, 18, GB3010, 10.1029/2004gb002239, 2004.

35 Zona, D., Gioli, B., Commane, R., Lindaas, J., Wofsy, S. C., Miller, C. E., Dinardo, S. J., Dengel, S., Sweeney, C., Karion, A., Chang, R. Y. W., Henderson, J. M., Murphy, P. C., Goodrich, J. P., Moreaux, V., Liljedahl, A., Watts, J. D., Kimball, J. S., Lipson, D. A., and Oechel, W. C.: Cold season emissions dominate the Arctic tundra methane budget, Proceedings of the National Academy of Sciences, 113, 40-45, 2016.

40

Table 1. Model parameter values for base scenario

Reaction	k_{max} (d^{-1})	k_D (μM)	k_{surf}	Reported k_{max} range
R1	0.83			
R2	0.5	12[1]	0.062[1]	0.96-2.16[2], 0.55 and 2.38[3], 0.34[4]
R3	0.8	11[1]	0.062[1]	
R4	0.3[5]	23[1]		
R5	0.5[5]	4.7[1]		
R6	0.05[5]			

[1] Jin, Q., and Roden, E. E.: Microbial physiology-based model of ethanol metabolism in subsurface sediments, J. Contam. Hydrol., 125, 1-12, 10.1016/j.jconhyd.2011.04.002, 2011.

[2] Esteve-Núñez, A., Rothermich, M., Sharma, M., and Lovley, D.: Growth of Geobacter sulfurreducens under nutrient-limiting conditions in continuous culture, Environmental Microbiology, 7, 641-648, 10.1111/j.1462-2920.2005.00731.x, 2005.

[3] Cord-Ruwisch, R., Lovley, D. R., and Schink, B.: Growth of Geobacter sulfurreducens with Acetate in Syntrophic Cooperation with Hydrogen-Oxidizing Anaerobic Partners, Applied and Environmental Microbiology, 64, 2232-2236, 1998.

[4] Holmes, D. E., Giloteaux, L., Barlett, M., Chavan, M. A., Smith, J. A., Williams, K. H., Wilkins, M., Long, P., and Lovley, D. R.: Molecular Analysis of the In Situ Growth Rates of Subsurface Geobacter Species, ibid., 79, 1646-1653, 2013.

[5] Rittmann, B. E., and McCarty, P. L.: Environmental biotechnology: principles and applications, McGraw-Hill, 2001.

Table 2. Experimental parameter values summarized from (Herndon et al., 2015;Roy Chowdhury et al., 2015).

Location	Horizon	Depth (cm)	pH	Soil (dwt g)	Water (g)	TOTC (g)	WEOC (mg)	Acetate (mgC)	Fe(II) (mmol)	Bulk den. (g/cm³)	Headspace (ml)
Center	Oa	6-21.5	5.02	1.412	13.588	0.542	9.585	2.079	0.0107	0.9106	42.5282
	Bgh	21.5-53.5	4.84	9.146	5.854	1.260	3.845	0.394	0.1302		
Ridge	Oe	0-8	5.21	3.212	11.788	1.249	6.790	0.016	0.0190	1.0003	44.0051
	Bh	8-42	4.54	8.621	6.379	1.263	3.282	0.409	0.1466		
Trough	Oe	0-19	5.23	4.310	10.690	0.886	3.324	0.022	0.1675	0.9724	43.5745
	Bh/ice	25-69	4.95	8.380	6.620	0.670	2.013	0.292	0.0475		

Figure 1: Extension of the CLM-CN decomposition cascade (Thornton and Rosenbloom, 2005) to include a LabileDOC pool. A portion of the original respiration fraction is assumed to produce LabileDOC, which undergoes fermentation, Fe reduction and methanogenesis to release CO_2 and CH_4. FeRB, MeGA, and MeGH denote microbial mass pools for Fe reducers, acetoclastic and hydrogenotrophic methanogens, respectively. τ is the turnover time.
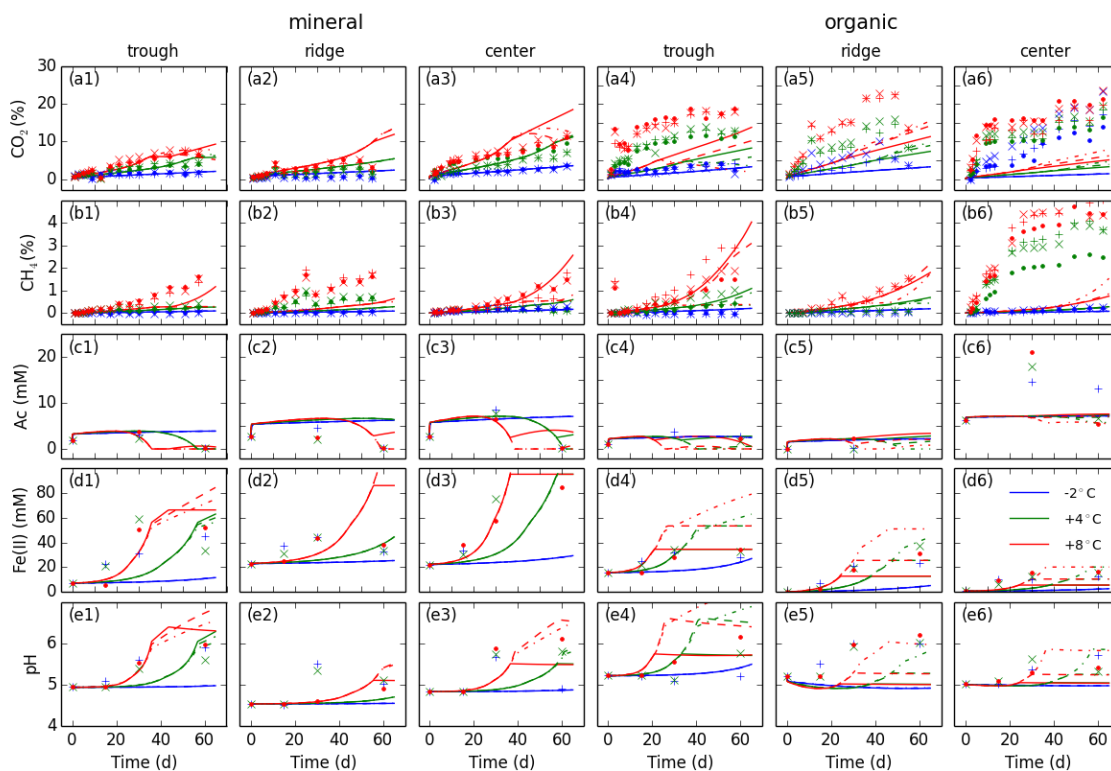
Figure 2: Comparison of observed and modeled CO$_2$ (a1-6) and CH$_4$ (b1-6) in the headspace, organic acid (Ac, c1-6), extractable Fe(II) (d1-6), and pH (e1-6) in the incubation tests with soils from an Arctic lower center polygon. Symbols represent observations with blue, green and red for -2, 4, and 8 °C. For CO$_2$ and CH$_4$, different symbols of the same color represent duplicates. The

5 **organic acids, such formate, acetate, propionate, and butyrate, reported by (Herndon et al., 2015) are combined as Ac in c1-6. The rest of the data were taken from (Roy Chowdhury et al., 2015). The curves are calculations based on model parameter values listed in Table 1 and experimental parameter values listed in Table 2. Trough, ridge, and center denote the microtopographic locations in the polygon, and mineral and organic denote soil horizons. Increasing the initial bioavailable Fe(III) f_{Fe} from 0.005 (continuous) to 0.1 (dash) and 0.02 (dashdot) brings the predictions close to the observations for Fe(II) and pH for center and ridge organic**

10 **soils.**
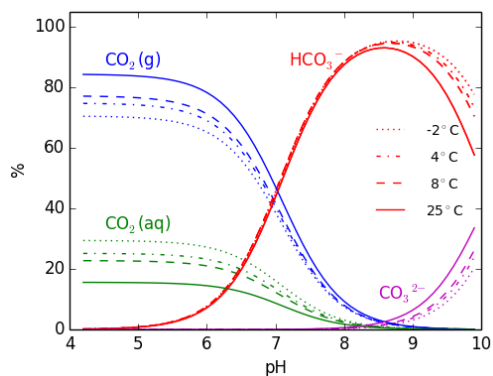
Figure 3: Partition of CO_2 among gas and aqueous phase species under various temperatures. The calculations are conducted with 45 ml headspace with N_2 and 10 ml solution with 10 mM total inorganic carbon using PHREEQC.
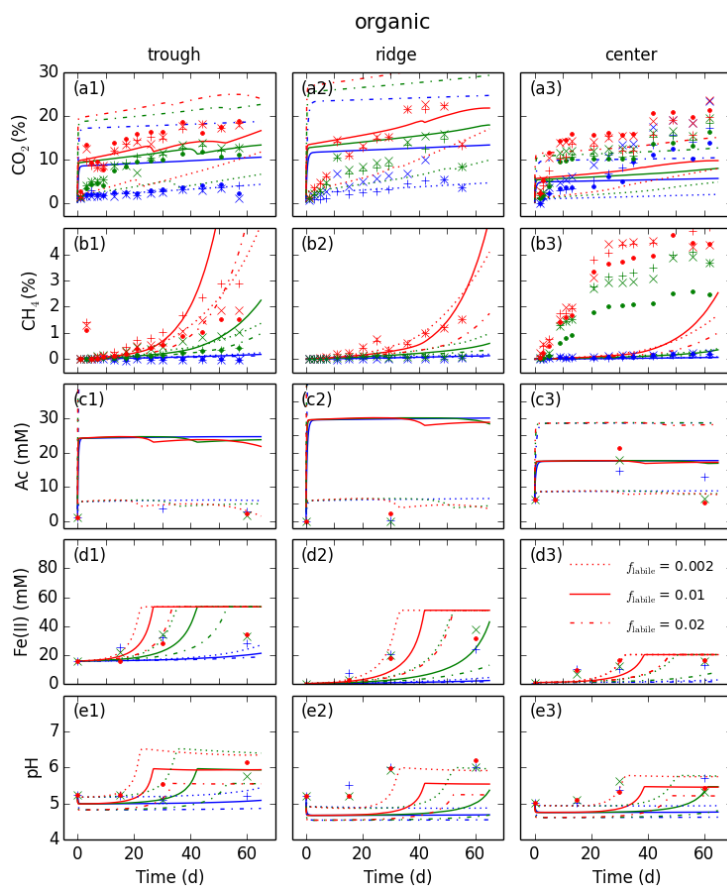
Figure 4: Increasing initial LabileDOC better describes the observed initial rapid CO$_2$ increase in the headspace for the organic soils.
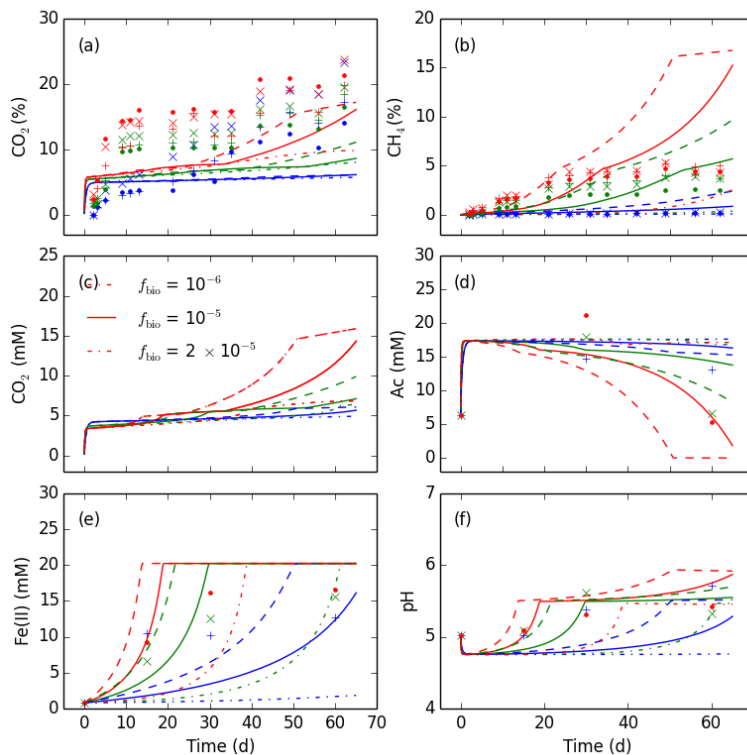
Figure 5: Increasing the initial biomass predicts rapid CH₄ accumulation at early times that is close to the observations but misses the level-off trend at late time for the center organic soils.
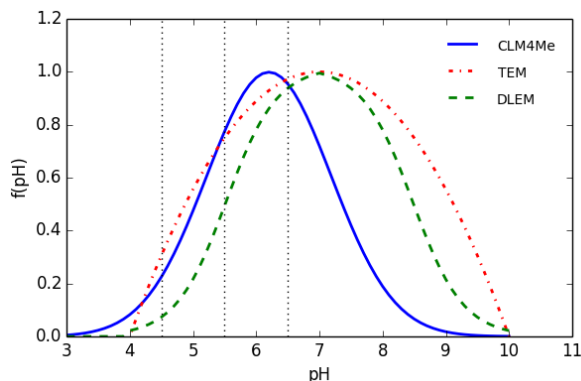
Figure 6: Comparison of pH response functions used in CLM4Me (Riley et al., 2011), TEM (Raich et al., 1991), and DLEM (Tian et al., 2010) as described by Eqs. 3, A1-3.
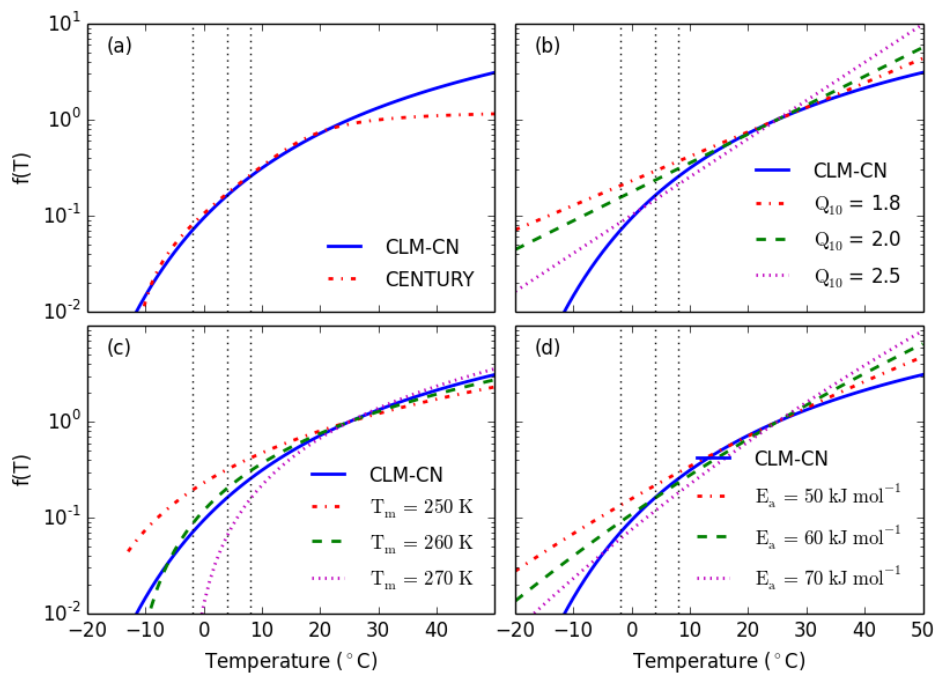
Figure 7: Comparison of temperature response functions used in (a) land surface models CLM-CN (Thornton and Rosenbloom, 2005), CENTURY (Parton et al., 2010), (b) Q_{10} (Oleson et al., 2013), (c) Ratkowsky equation (Ratkowsky et al., 1982) and (d) Arrhenius equation (Wang et al., 2013) described by Eq. (4, B1-B4).